Appendix F

Evaluating the Effect of the North Delta Diversion on Flow Reversals and Entrainment of Juvenile Chinook Salmon into Georgiana Slough and the Delta Cross Channel

USGS
science for a changing world

Prepared in cooperation with National Atmospheric and Oceanic Administration, National Marine Fisheries Service

Evaluating the Effect of the North Delta Diversion on Flow Reversals and Entrainment of Juvenile Chinook Salmon into Georgiana Slough and the Delta Cross Channel

By Russell W. Perry, Jason G. Romine, Adam C. Pope, and Scott D. Evans

Open File Report 2016–XXXX

U.S. Department of the Interior
U.S. Geological Survey

U.S. Department of the Interior
Sally Jewel, Secretary

U.S. Geological Survey
Suzette Kimball, Acting Director

U.S. Geological Survey, Reston, Virginia 2016

For product and ordering information:
World Wide Web: http://www.usgs.gov/pubprod
Telephone: 1-888-ASK-USGS

For more information on the USGS—the Federal source for science about the Earth,
its natural and living resources, natural hazards, and the environment:
World Wide Web: http://www.usgs.gov
Telephone: 1-888-ASK-USGS

Suggested citation: Perry, R.W., Romine, J.G., Pope, A.C., and Evans, S.D., 2016, Evaluating the Effect of the North Delta Diversion on Flow Reversals and Entrainment of Juvenile Chinook Salmon into Georgiana Slough and the Delta Cross Channel: U.S. Geological Survey Open file Report 2016-XXXX,XX p.

Contents

Figures

Tables

Conversion Factors

Inch/Pound to SI

Multiply	By	To obtain
	Length	
inch (in.)	2.54	centimeter (cm)
foot (ft)	0.3048	meter (m)
mile (mi)	1.609	kilometer (km)
	Area	
acre	0.4047	square hectometer (hm^2)
acre	0.004047	square kilometer (km^2)
square foot (ft^2)	0.09290	square meter (m^2)
square mile (mi^2)	259.0	hectare (ha)
square mile (mi^2)	2.590	square kilometer (km^2)
	Volume	
cubic foot (ft^3)	0.02832	cubic meter (m^3)
	Flow rate	
cubic foot per second (ft^3/s)	0.02832	cubic meter per second (m^3/s)

Temperature in degrees Celsius (°C) may be converted to degrees Fahrenheit (°F) as follows:

°F=(1.8×°C)+32

Temperature in degrees Fahrenheit (°F) may be converted to degrees Celsius (°C) as follows:

°C=(°F-32)/1.8

Vertical coordinate information is referenced to the insert datum name (and abbreviation) here for instance, “North American Vertical Datum of 1988 (NAVD 88).”

Horizontal coordinate information is referenced to the insert datum name (and abbreviation) here for instance, “North American Datum of 1983 (NAD 83).”

Altitude, as used in this report, refers to distance above the vertical datum.

Evaluating the Effect of the North Delta Diversion on Flow Reversals and Entrainment of Juvenile Chinook Salmon into Georgiana Slough and the Delta Cross Channel

By Russell W. Perry, Jason G. Romine, Adam C. Pope, and Scott D. Evans

Executive Summary

The California Department of Water Resources and US Bureau of Reclamation propose new water intake facilities on the Sacramento River that would route water through tunnels rather than through the Sacramento-San Joaquin Delta. The collection of water intakes, tunnels, pumping facilities, associated structures, and proposed operations are collectively referred to as California Water Fix (ICF International, 2016). The water intake facilities, referred to here as the North Delta Diversion (NDD), are proposed to be located on the Sacramento River downstream of the city of Sacramento but upstream of the first major river junction where Sutter Slough branches from the Sacramento River. The North Delta Diversion can divert a maximum discharge of 9,000 ft^3/s from the Sacramento River, which reduces the amount of inflow into the Delta.

In this report, we conduct two analyses to investigate the effect of the North Delta Diversion and its proposed operation on entrainment of juvenile Chinook salmon (*Oncorhynchus tshawytscha*) into Georgiana Slough and the Delta Cross Channel. Fish that enter the interior Delta (the network of channels to the south of the Sacramento River) via Georgiana Slough and the Delta Cross Channel survive at lower rates than fish that use other migration routes (Sacramento River, Sutter Slough, and Steamboat Slough; Perry and others 2010). Therefore, of concern is the extent to which operation of the North Delta Diversion increases the proportion of the population entering the interior Delta, which would lower overall survival through the Delta by increasing the fraction of the population subject to lower survival rates.

In the first analysis, we evaluate the effect of the NDD bypass rules on flow reversals of the Sacramento River below Georgiana Slough. The NDD bypass rules are a set of operational criteria designed to minimize upstream transport of fish into Georgiana Slough and Delta Cross Channel, and were developed based on previous studies showing that the magnitude and duration of flow reversals increase the proportion of fish entering Georgiana Slough and the Delta Cross Channel (Perry and others, 2015; Perry, 2010). We estimated the frequency and duration of reverse-flow conditions of the Sacramento River downstream of Georgiana Slough under each of the prescribed minimum bypass flows described in the NDD bypass rules. To accommodate adaptive levels of protection during different times of year when juvenile salmon are migrating through the Delta, the NDD bypass rules prescribe a series of minimum allowable bypass flows that vary depending on 1) month of the year and 2) progressively decreasing levels of protection following a pulse flow event.

We found that the NDD bypass rules increased the frequency and duration of reverse flows of the Sacramento River downstream of Georgiana Slough, with the magnitude of increase varying among scenarios. Constant low-level pumping, the most protective bypass rule that limits diversion to 10% of the maximum diversion and is implemented following a pulse-flow event, led to the smallest increase in

frequency and duration of flow reversals. In contrast, we found that some scenarios led to sizeable increases in the fraction of the day with reverse flow. The conditions under which the proportion of the day with reverse flow can increase by ≥10 percentage points between October and June, when juvenile salmon are present in the Delta, include October–November bypass rules and level 3 post-pulse operations from December through June. These conditions would be expected to increase the proportion of juvenile salmon entering the interior Delta via Georgiana Slough.

In the second analysis, we evaluated the effect of the North Delta Diversion on the daily probability of fish entering Georgiana Slough and Delta Cross Channel. We applied the entrainment probability model of Perry and others (2015) to 15-minute flow data for an 82-year time series of flows simulated by DSM2 (Delta Simulation Model 2) under the Proposed Action (PA) and the No Action Alternative (NAA). To estimate the daily fraction of fish entering each river channel, entrainment probabilities were averaged over each day. To evaluate the two scenarios, we then compared mean annual entrainment probabilities by month, water year classification, and three different assumed run timings.

Effect of the North Delta Diversion Bypass Rules on Flow Reversal of the Sacramento River below Georgiana Slough

Introduction

This analysis investigates the effects of the North Delta Diversion (NDD) bypass rules (Table 3.4.1–2 in DWR, 2013) on the frequency and duration of reverse flows of the Sacramento below Georgiana Slough. One goal of the NDD bypass rules is to provide bypass flows that prevent an increase in upstream transport of fish into Georgiana Slough and the Delta Cross Channel (DCC). Bypass flows are defined as flow remaining in the Sacramento River downstream of the North Delta Diversion. These rules were developed based on previous research and understanding of reverse-flow hydrodynamics at this river junction. Research has shown that the entrainment probability of juvenile Chinook salmon (*Oncorhynchus tshawytscha*) into Georgiana Slough and the Delta Cross Channel is highest during reverse-flow flood tides (Perry and others, 2015). Furthermore, the daily proportion of fish entrained into Georgiana Slough increases with the fraction of the day in a reverse flow condition at the Sacramento River downstream of Georgiana Slough (Perry, 2010). Consequently, diverting water from the Sacramento River could increase the frequency and duration of reverse-flow conditions, thereby reducing survival by increasing the proportion of fish entrained into the interior Delta where survival probabilities are lower than in the Sacramento River (Perry and others, 2010, 2013).

The NDD bypass rules are also designed to provide more protection during times of the year when juvenile salmon populations are actively migrating through the Delta (primarily December through June) and during pulse flow events when endangered winter-run Chinook salmon are likely to initiate downstream migration into the Delta (del Rosario and others, 2013). To accommodate adaptive levels of protection, the NDD bypass rules prescribe a series of minimum allowable bypass flows that vary depending on 1) month of the year and 2) progressively decreasing levels of protection following a pulse flow event. For modeling purposes, pulse-events are defined based on discharge of the Sacramento River at Wilkins Slough, and minimum bypass levels are based on varying fractions of discharge of the Sacramento River arriving at the North Delta Diversion (see Table 3.4.1–2 in DWR, 2013 for details). For operational purposes, pulse events will be based on monitoring for the presence of winter-run sized fish entering the reach.

Our goal was to estimate the frequency and duration of reverse-flow conditions of the Sacramento River downstream of Georgiana Slough under each of the prescribed minimum bypass flows described in the NDD bypass rules Table 3.4.1–2. First, we used historical flow data of the Sacramento River downstream of Georgiana Slough (WGB; USGS Gage 11447905) to estimate the effect of discharge of the Sacramento River at Freeport (FPT; USGS Gage 11447650) on 1) the daily probability of a flow reversal, and 2) the daily proportion of each day with reverse flow. We then used these relationships to calculate the change in the probability of a flow reversal and the proportion of the day with reverse flow under each of the prescribed bypass flows described in the NDD bypass rules. This analysis assumes that 1) the NDD bypass rules are applied based on mean daily discharge at Freeport, and 2) that water is diverted at a constant discharge over an entire day such that the bypass flow is constant over the day. In other words, we assume that the bypass is operated as strictly defined by the NDD bypass rules. We do not attempt to simulate "real time management" such as varying diversion flow at hourly timescales in response to in situ tidal conditions to prevent reverse flows. Such real-time management criteria have yet to be defined, and we therefore expand on this topic in the discussion.

Methods

We used logistic regression to quantify the relationship between Sacramento River inflows to the Delta and reverse flows of the Sacramento River downstream of Georgiana Slough. Mean daily discharge at Freeport, 15-min discharge data at station WGB, and the daily position of the Delta Cross Channel (DCC) gate for the period October 2007 to March 2015 were used in the analysis. The 15-min data at WGB was summarized to two daily statistics: 1) a binary indicator value that was set to one if reverse flow occurred at any point on a given day and set to zero if all 15-min flows were positive, and 2) the number of 15-min flow observations for each day that were negative. The position of the DCC gate was coded as a binary indicator variable (1 = open, 0 = closed) for inclusion in the analysis. Dates without a complete record of 15-min flows at WGB or where the DCC gate was not open or closed for the entire day were excluded from the analysis.

To estimate the probability of a flow reversal occurring on a given day, we fit a logistic regression model to the binary indicator variable described above as a function of daily flow at Freeport:

$$P(\text{reverse}) = \text{logit}^{-1}(\alpha_0 + \alpha_1 Q_{FPT})$$

where logit^{-1} is the inverse logit function, Q_{FPT} is mean daily discharge at Freeport, α_0 is the intercept, and α_1 is the slope. We excluded the DCC gate position from this analysis because we found that flow reversals always occurred for some part of the day when the DCC was open (i.e., P(reverse) = 1 for DCC open). Therefore, the analysis was restricted to days when the DCC was closed.

To estimate the proportion of the day with reverse flow as a function of Freeport flow, we fit a logistic regression model to the number of 15-min reverse flows on each day relative to the total number 15-min flow observations each day:

$$P_{day}(\text{reverse}) = \text{logit}^{-1}(\beta_0 + \beta_1 Q_{FPT})$$

where β_0 is the intercept and β_1 is the slope. This analysis was conducted separately for periods with the DCC gate open and closed.

Given the relationships estimating the effect of Freeport discharge on the frequency (P(reverse)) and duration (P_{day}(reverse)) of flow reversals, we applied the bypass rules over a range of Freeport discharge from 5,000 to 35,000 ft^3/s, which bracketed flows under which we observed a 100% probability of a flow reversal to a 0% probability of a flow reversal. We compared the probability of flow reversal and the proportion of the day with flow reversals assuming no diversion and diversion under the NDD bypass rules with the DCC closed. We then calculated the difference in these statistics

between no diversion and that prescribed under the NDD bypass rules to assess the magnitude of increase in the frequency and duration of reverse flows. Specifically, we performed this comparison for the 12 scenarios described under the NDD bypass rules:

1) Constant low-level pumping
2) October–November bypass rules
3) Level 1, 2, and 3 post-pulse operations for December–April
4) Level 1, 2, and 3 post-pulse operations for May
5) Level 1, 2, and 3 post-pulse operations for June
6) July–September bypass rules

Results

We found the probability of a flow reversal declined from one at about 12,500 ft^3/s to zero at about 22,500 ft^3/s (fig. 1). We found that the proportion of day with negative flow was about 45 percent at a Freeport discharge of about 6,000 ft^3/s regardless of the DCC gate position (fig. 2). However, DCC gate position had a strong effect on the rate of change in the proportion of the day with reverse flows (table 1). As Freeport discharge increased over 6,000 ft^3/s, the fraction of the day with reverse flows decreased much more sharply with the DCC closed relative to open (fig. 2).

Table 1. Parameter estimates for the three logistic regression models used to estimate frequency and duration of flow reversals of the Sacramento River downstream of Georgiana Slough as a function of mean daily discharge at Freeport.

[DCC, Delta Cross Channel; SE, standard error; P, probability]

Response variable	DCC position	Intercept (SE)	Slope (SE)
P(reverse)	Closed	17.92 (1.567)	-1.017e-03 (9.001e-05)
P_{day}(reverse)	Closed	0.13 (0.022)	-5.837e-05 (1.600e-06)
	Open	1.37 (0.027)	-2.409e-04 (2.477e-06)

We found that the NDD bypass rules, as implemented under the assumptions of our simulation, increased the frequency and duration of reverse flows of the Sacramento River downstream of Georgiana Slough, with the magnitude of increase varying among scenarios (figs. 2–13). Constant low-level pumping, the most protective bypass rule, led to the smallest increase in frequency and duration of flow reversals (fig. 2). For example, the probability of a flow reversal increased by a maximum of 22 percentage points at a Freeport discharge of 18,000 ft^3/s, but the maximum increase in the proportion of the day with reverse flow increased by only 2.9 percentage points at a Freeport discharge of 10,000 ft^3/s. In contrast, in December–April when most populations of juvenile salmon are migrating through the Delta, level 3 post-pulse operations led to sizeable increases in the frequency and duration of flow reversals (fig. 6). Under these conditions, the probability of a flow reversal occurring increased from a 1 percent chance to a 99 percent chance at Freeport flows of 22,000 ft^3/s. More importantly, at this discharge, the proportion of each day with reverse flow increased by 12 percentage points from 0.019 to 0.146 (fig. 6). These conditions would be expected to increase the proportion of juvenile salmon entering Georgiana Slough.

Juvenile salmon are also present in the Delta, albeit at lower abundances, during other periods with less restrictive bypass rules (e.g., May, and October–November). Under October–November bypass rules, the proportion of the day with reverse flow increased by a maximum of 34 percentage points at a Freeport discharge of 16,000 ft^3/s (fig. 3). Under level 3 post-pulse operations in May, the

proportion of the day with reverse flow is expected to increase by a maximum of 14.3 percentage points at a Freeport discharge of 21,400 ft^3/s.

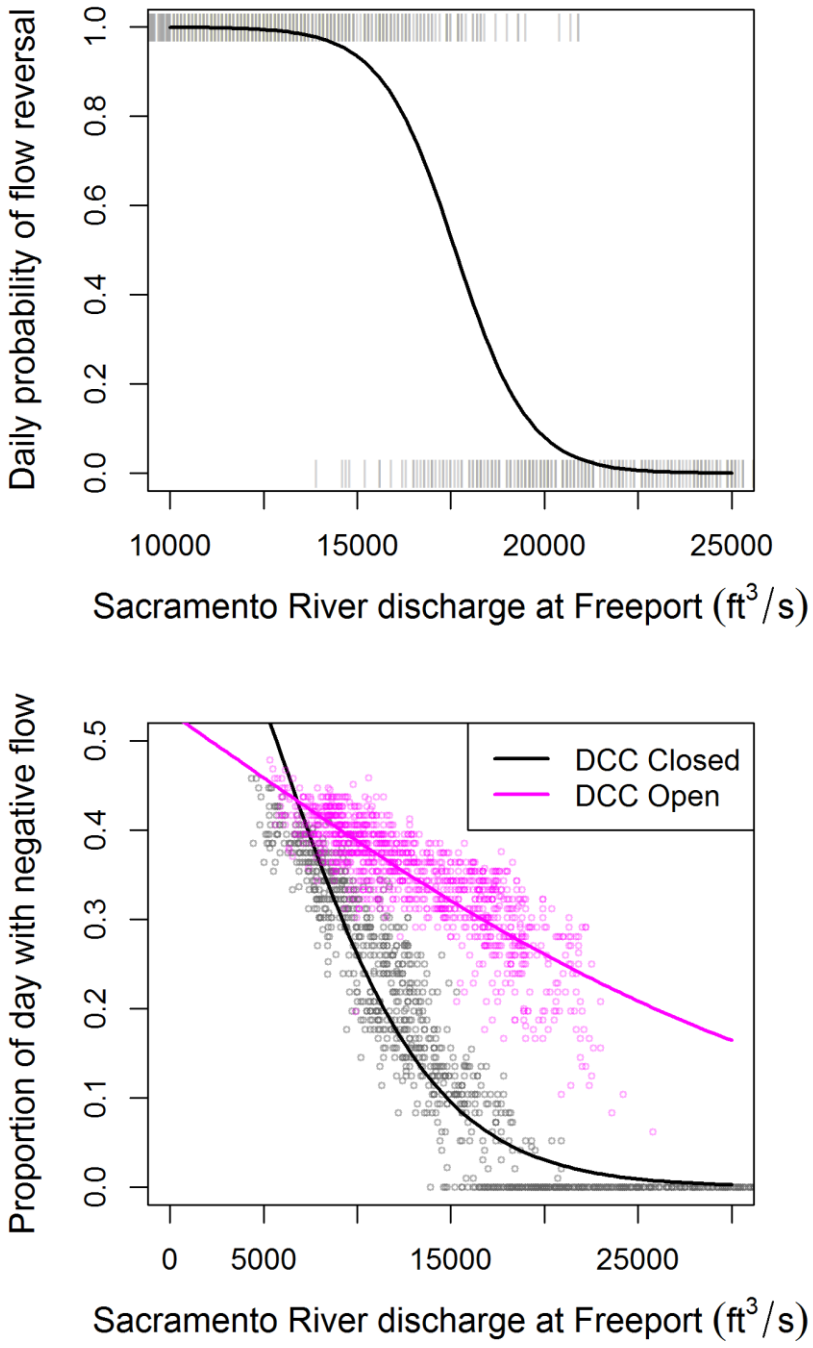

Figure 1. Effect of discharge at Freeport on frequency and duration of flow reversals. Top panel shows the effect of the mean daily discharge (cfs; cubic feet per second) at Freeport on the probability of a flow reversal occurring on a given day at the USGS gage in the Sacramento River just downstream of Georgiana Slough with the Delta Cross Channel (DCC) gate closed. The bottom panel shows the fraction of each day with reversing flow as a function of DCC gate position and mean daily discharge at Freeport.

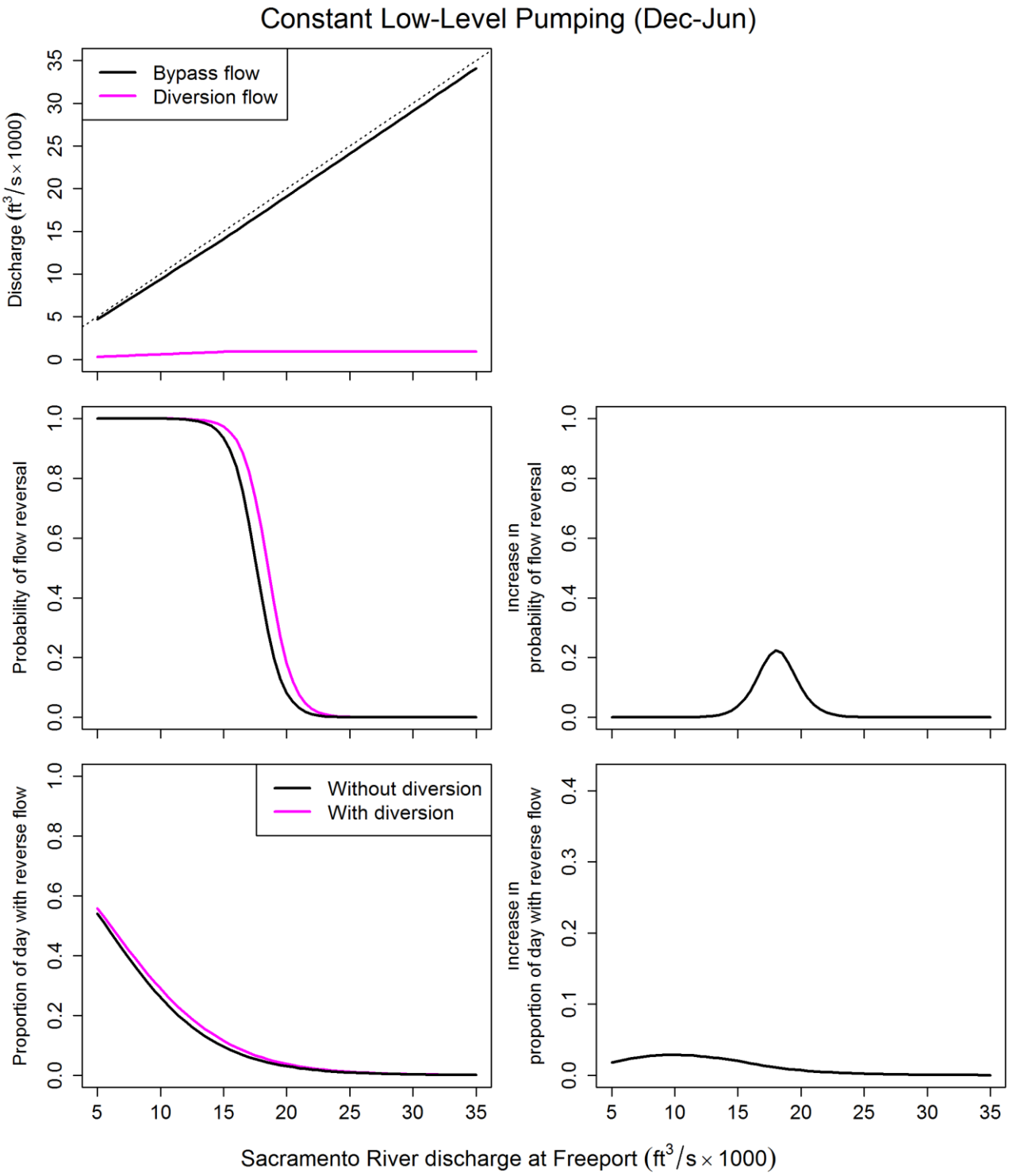

Figure 2. Effect of North Delta Diversion (NDD) on bypass discharge, probability of flow reversal, and proportion of the day with reverse flow for constant low-level pumping as defined in the NDD bypass rules. In the top panel, the dotted line shows bypass discharge when diversion discharge is zero.

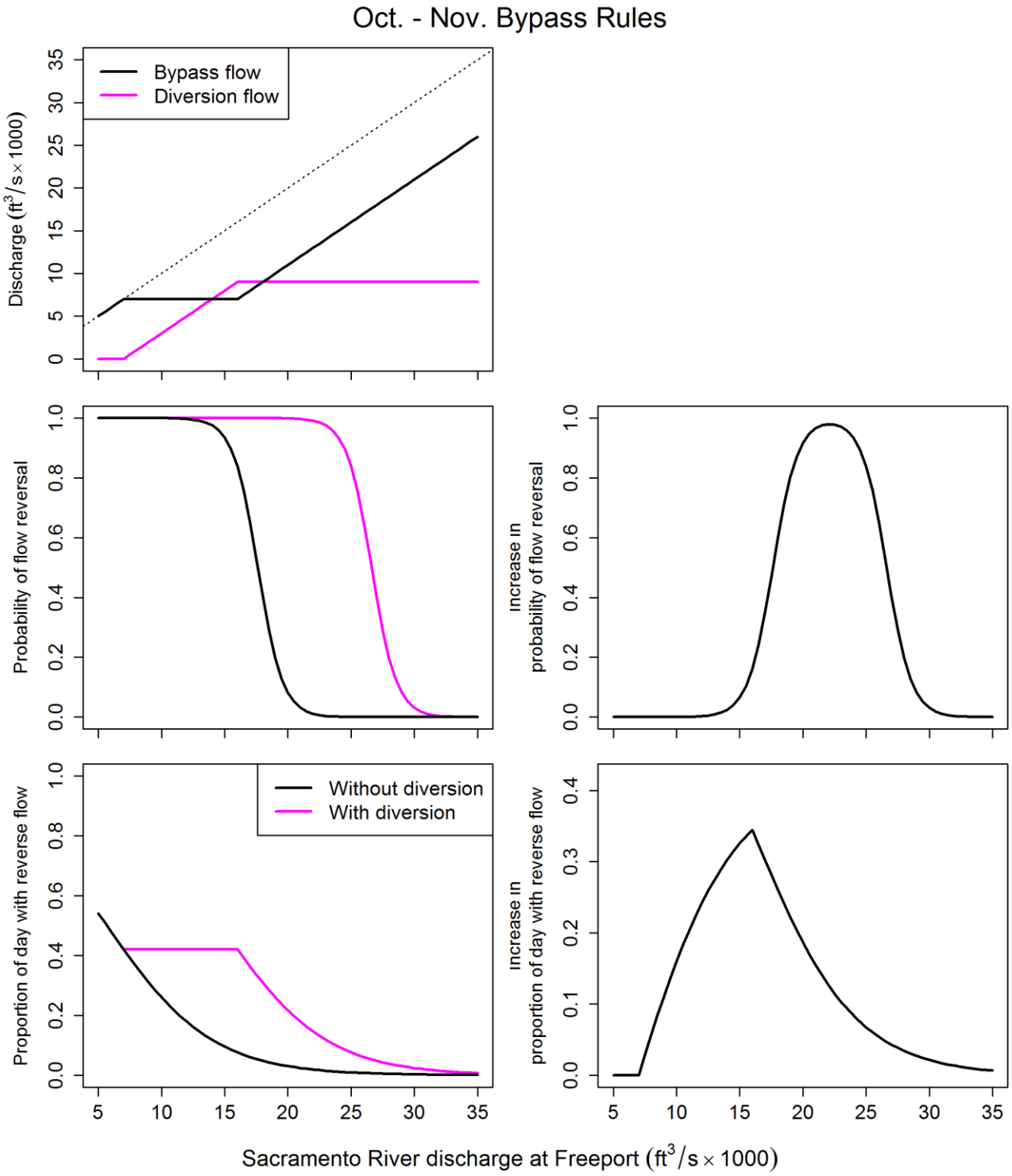

Figure 3. Effect of North Delta Diversion (NDD) on bypass discharge, probability of flow reversal, and proportion of the day with reverse flow for October–November as defined in the NDD bypass rules. In the top panel, the dotted line shows bypass discharge when diversion discharge is zero.

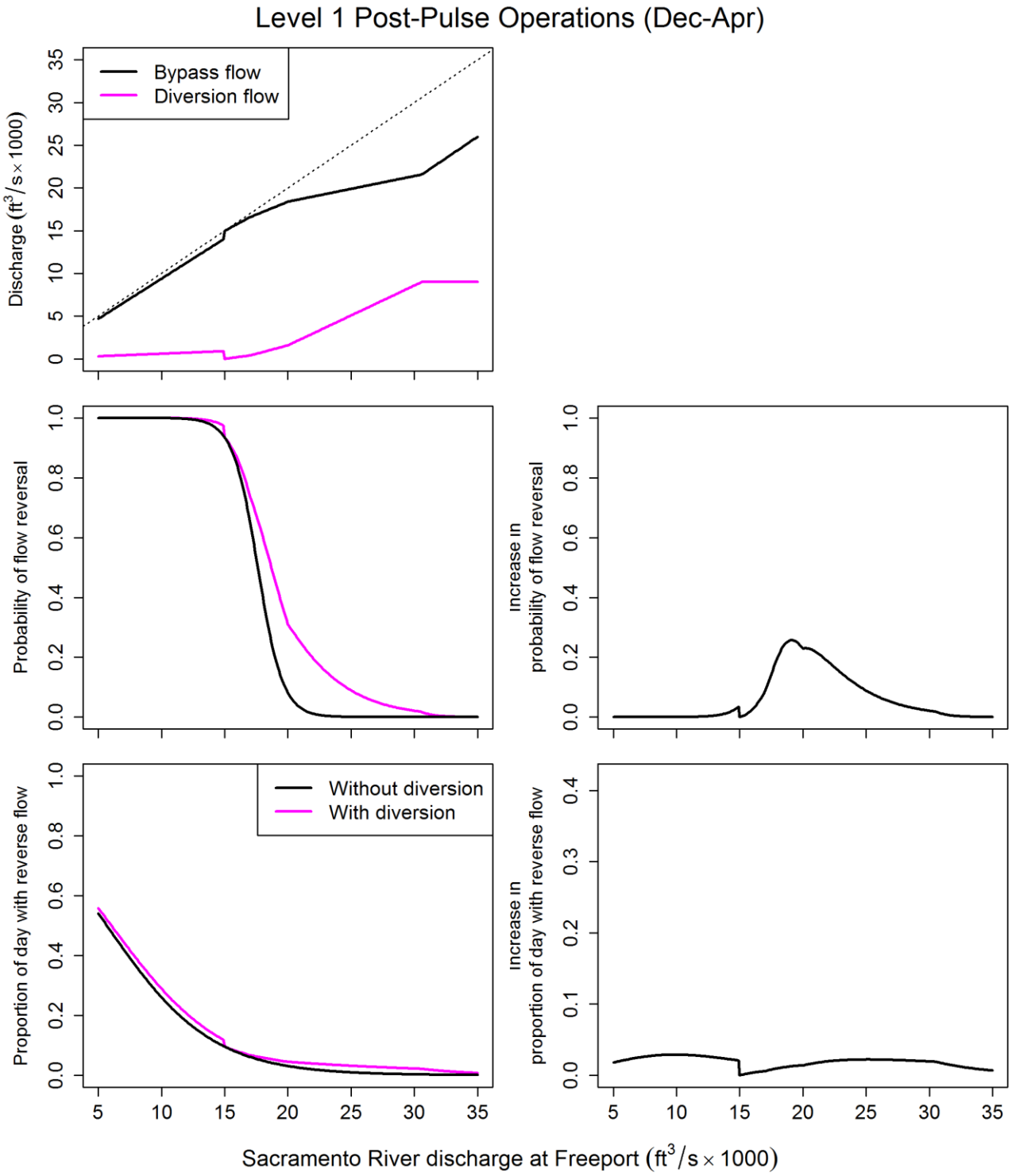

Figure 4. Effect of North Delta Diversion (NDD) on bypass discharge, probability of flow reversal, and proportion of the day with reverse flow for Level 1 post-pulse operations in December–April as defined in the NDD bypass rules. In the top panel, the dotted line shows bypass discharge when diversion discharge is zero.

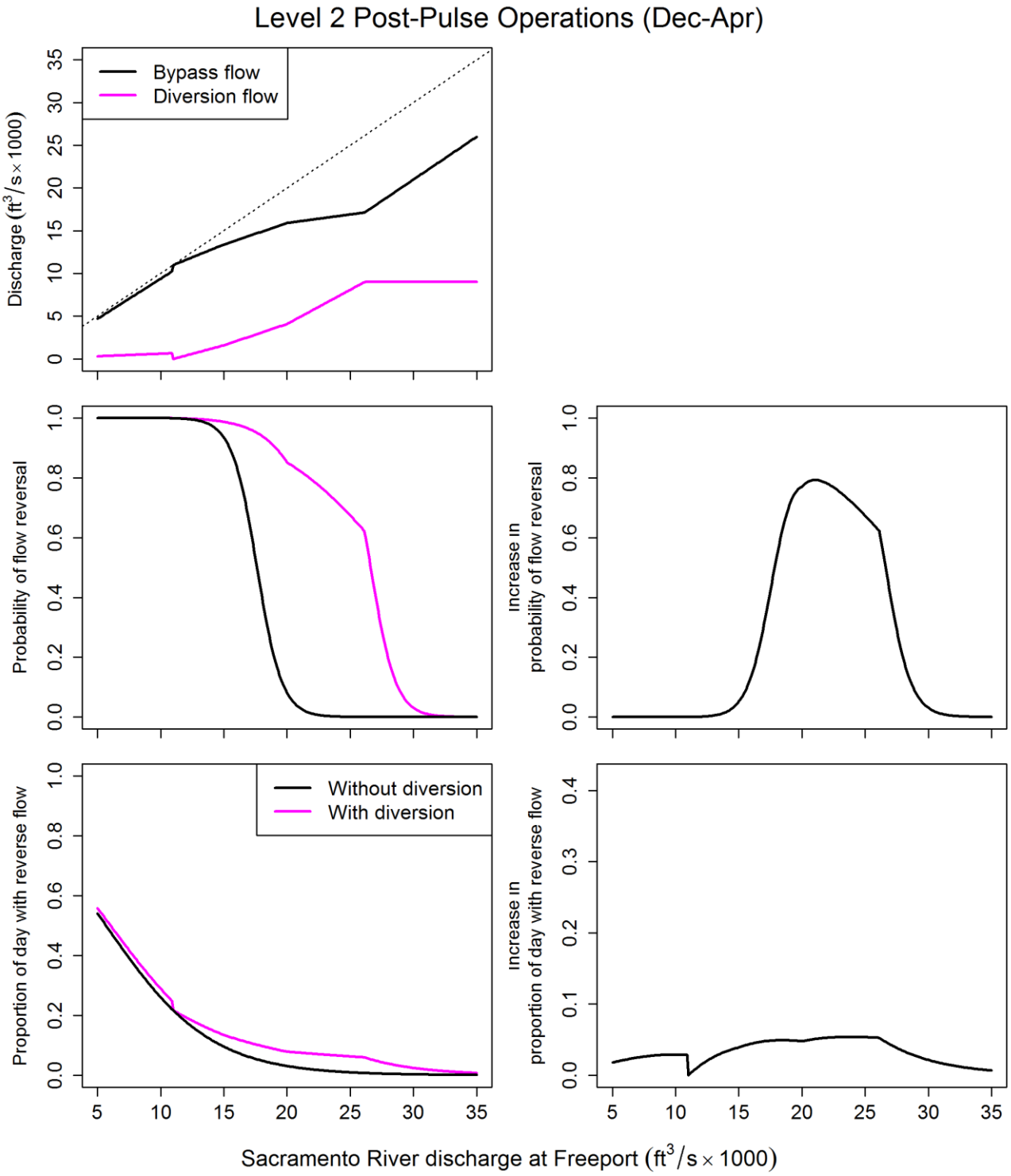

Figure 5. Effect of North Delta Diversion (NDD) on bypass discharge, probability of flow reversal, and proportion of the day with reverse flow for Level 2 post-pulse operations in December–April as defined in the NDD bypass rules. In the top panel, the dotted line shows bypass discharge when diversion discharge is zero.

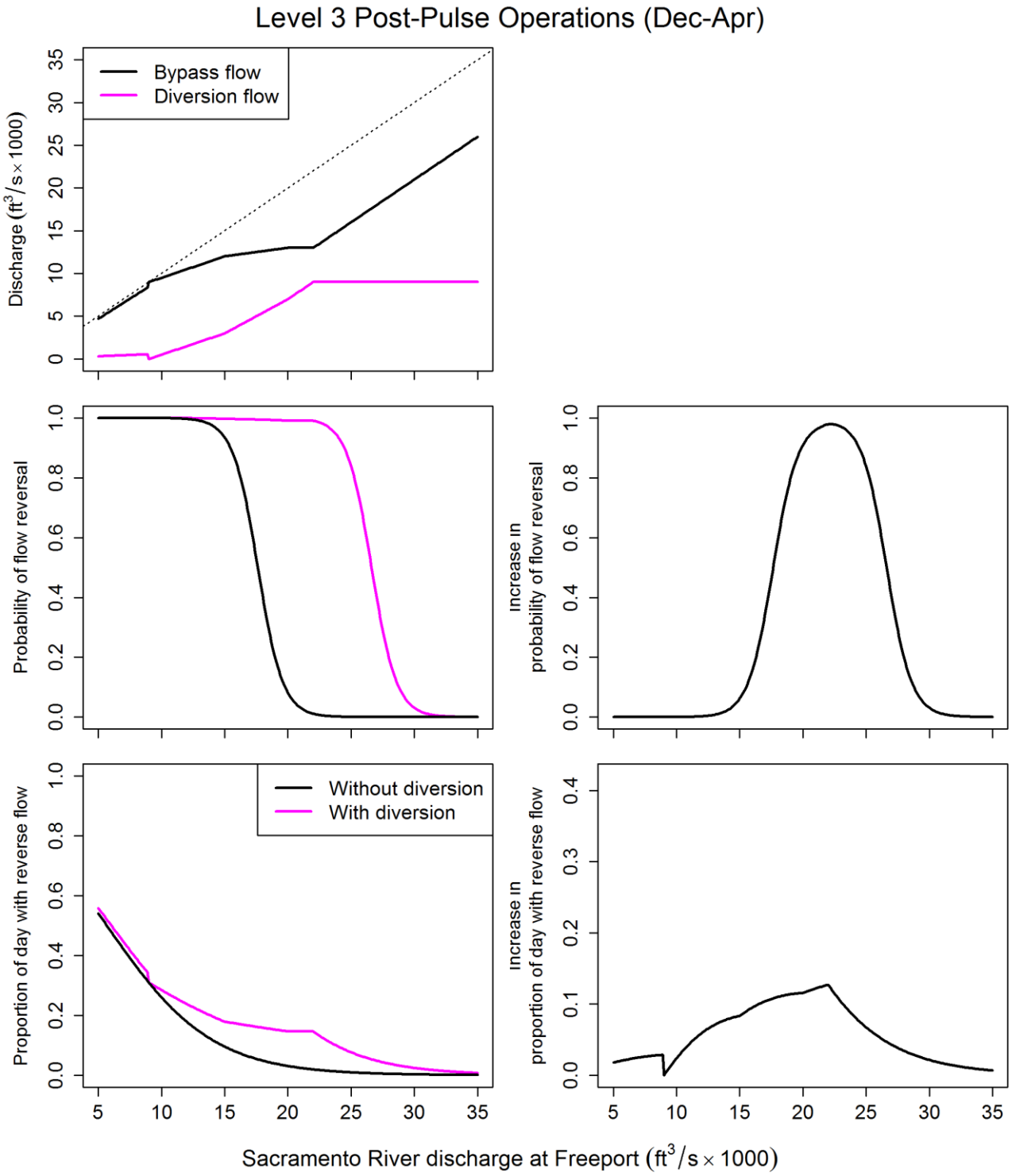

Figure 6. Effect of North Delta Diversion (NDD) on bypass discharge, probability of flow reversal, and proportion of the day with reverse flow for Level 3 post-pulse operations in December–April as defined in the NDD bypass rules. In the top panel, the dotted line shows bypass discharge when diversion discharge is zero.

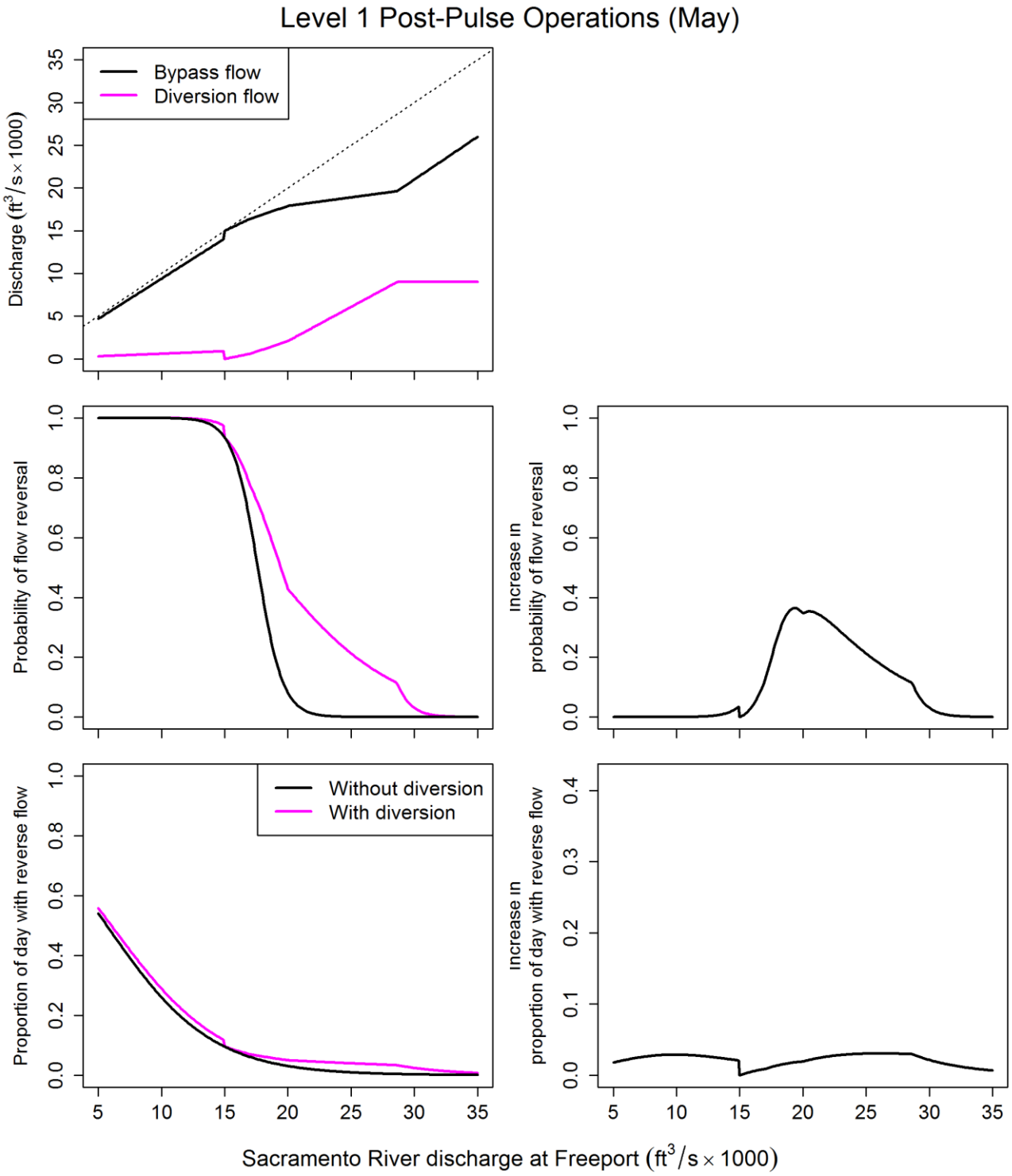

Figure 7. Effect of North Delta Diversion (NDD) on bypass discharge, probability of flow reversal, and proportion of the day with reverse flow for Level 1 post-pulse operations in May as defined in the NDD bypass rules. In the top panel, the dotted line shows bypass discharge when diversion discharge is zero.

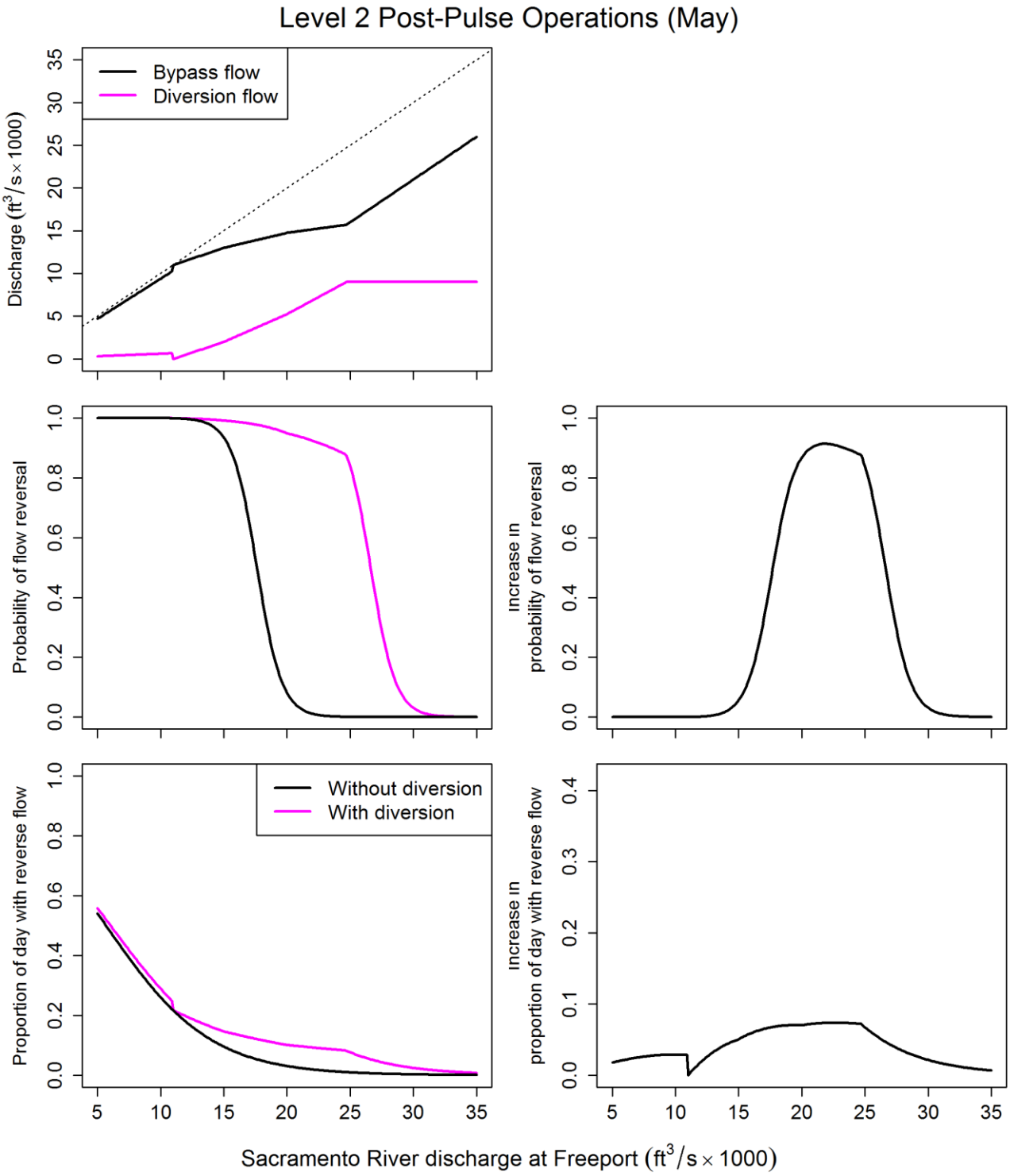

Figure 8. Effect of North Delta Diversion (NDD) on bypass discharge, probability of flow reversal, and proportion of the day with reverse flow for Level 2 post-pulse operations in May as defined in the NDD bypass rules. In the top panel, the dotted line shows bypass discharge when diversion discharge is zero.

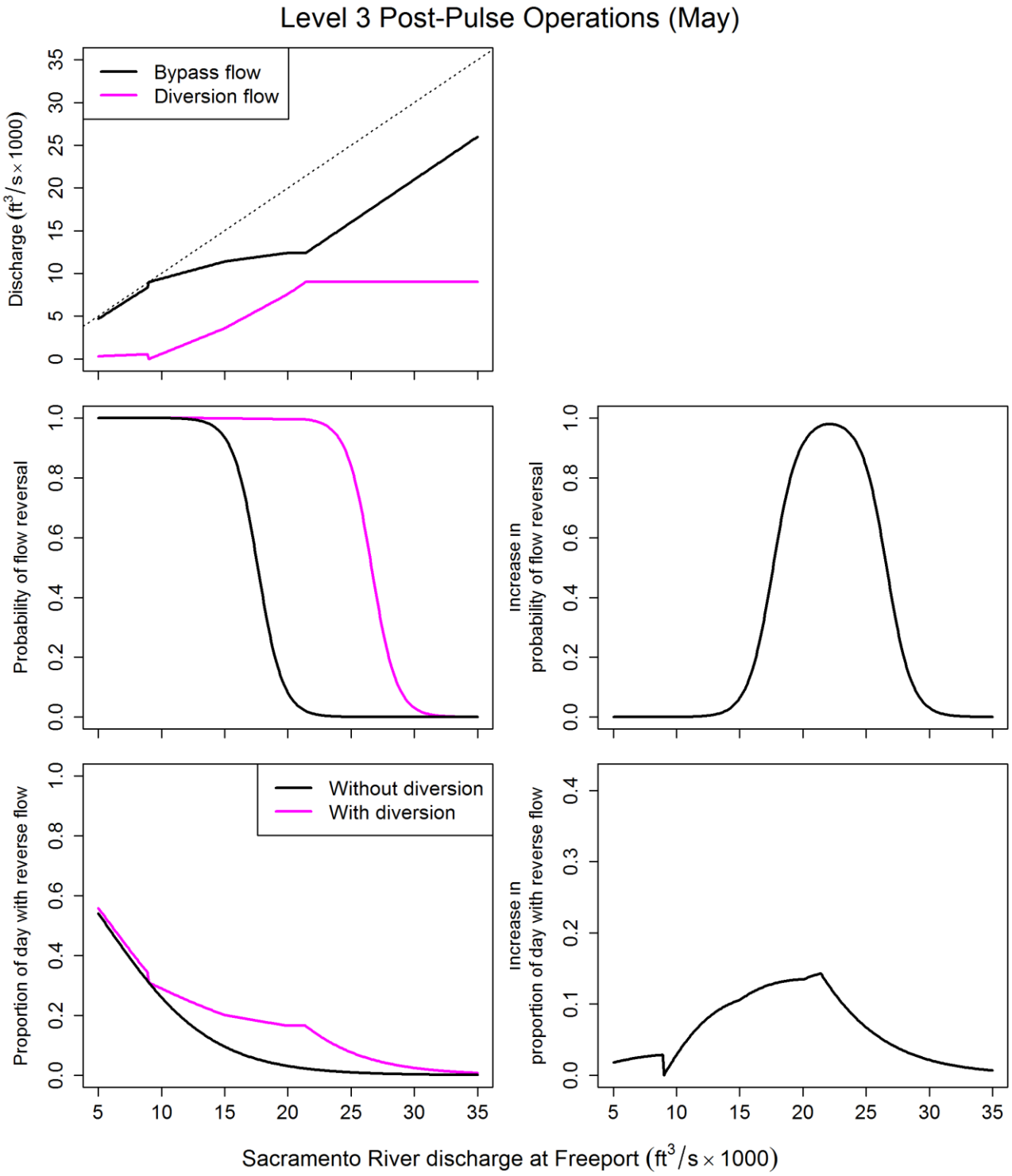

Figure 9. Effect of North Delta Diversion (NDD) on bypass discharge, probability of flow reversal, and proportion of the day with reverse flow for Level 3 post-pulse operations in May as defined in the NDD bypass rules. In the top panel, the dotted line shows bypass discharge when diversion discharge is zero.

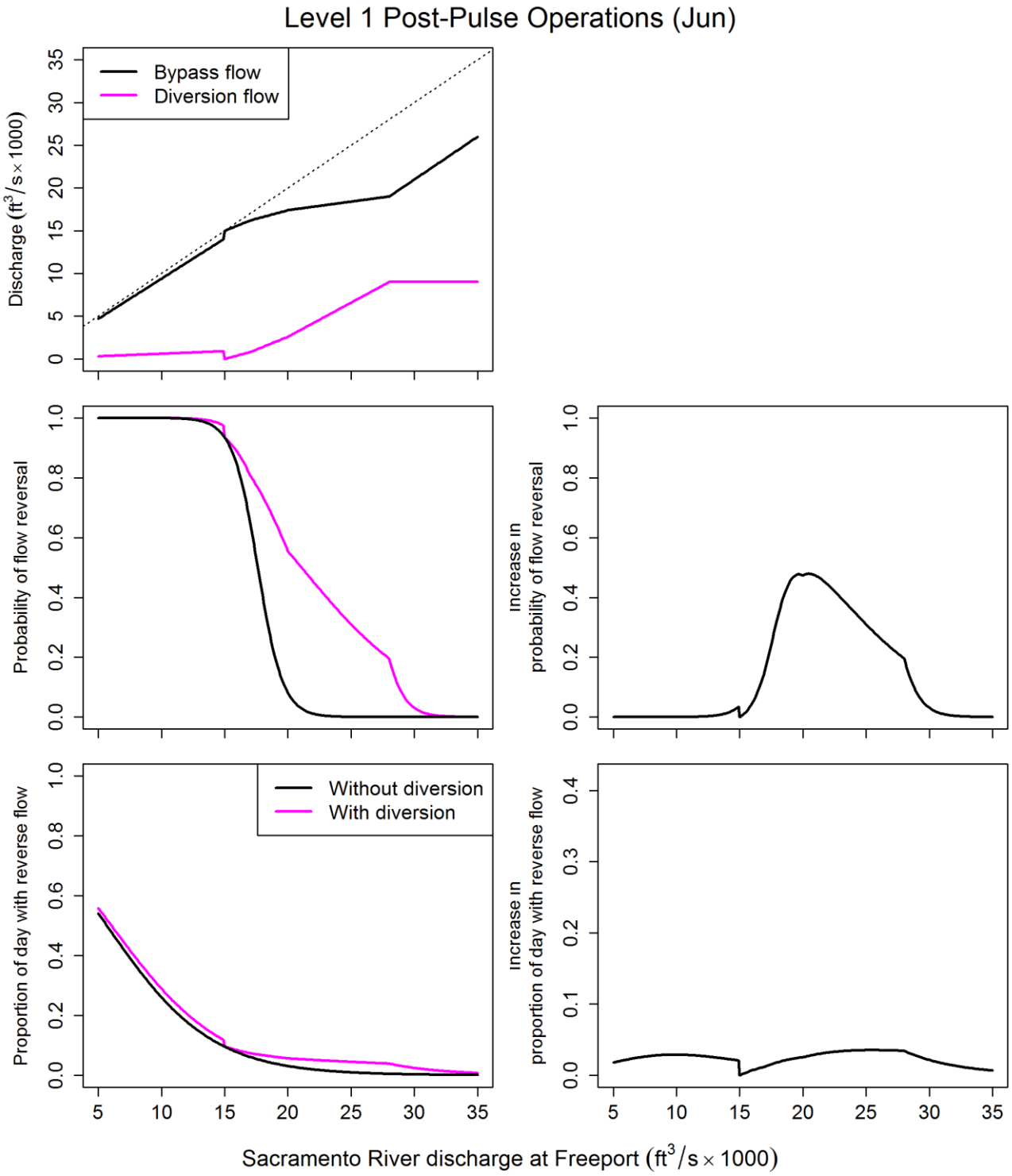

Figure 10. Effect of North Delta Diversion (NDD) on bypass discharge, probability of flow reversal, and proportion of the day with reverse flow for Level 1 post-pulse operations in June as defined in the NDD bypass rules. In the top panel, the dotted line shows bypass discharge when diversion discharge is zero.

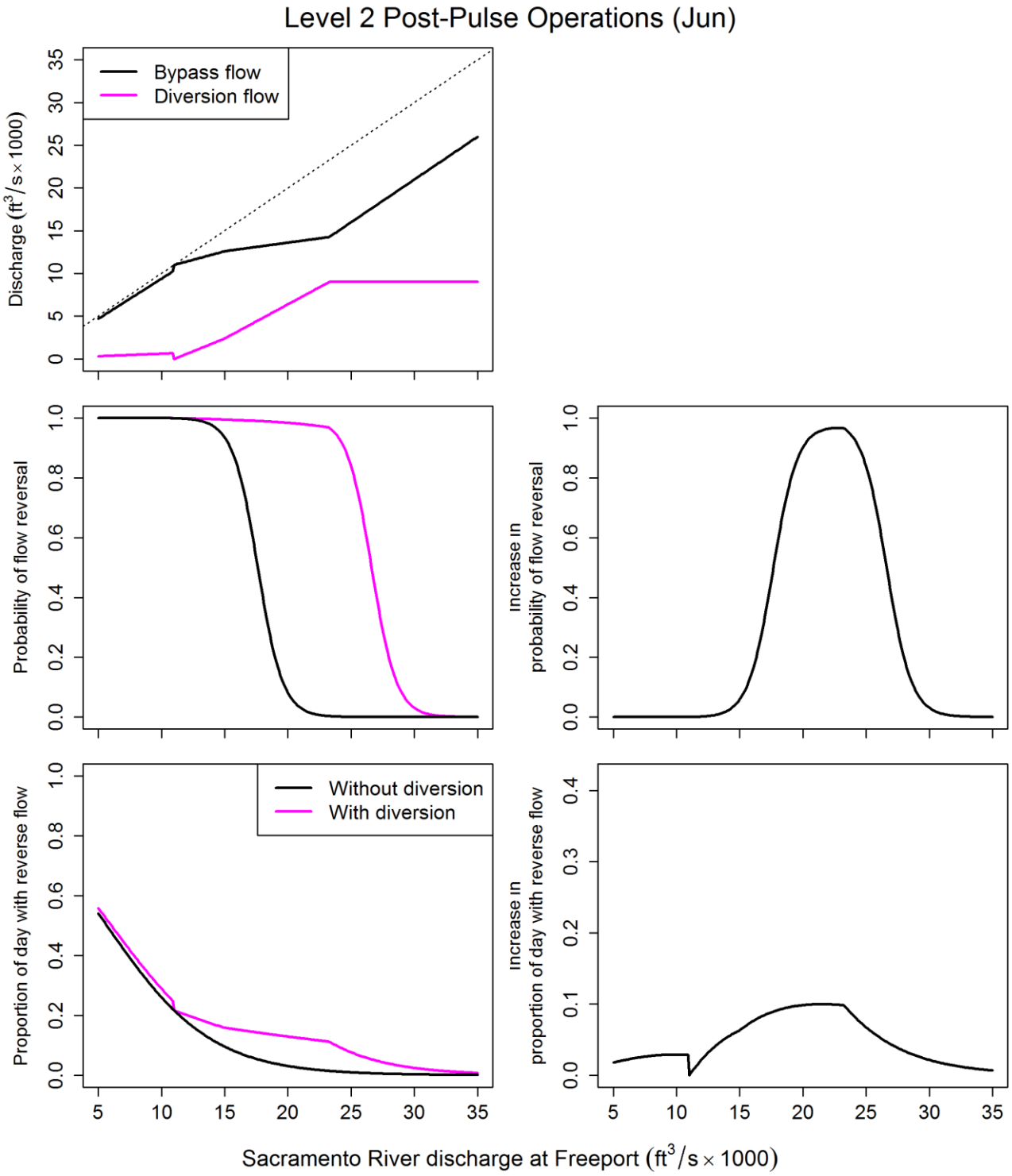

Figure 11. Effect of North Delta Diversion (NDD) on bypass discharge, probability of flow reversal, and proportion of the day with reverse flow for Level 2 post-pulse operations in June as defined in the NDD bypass rules. In the top panel, the dotted line shows bypass discharge when diversion discharge is zero.

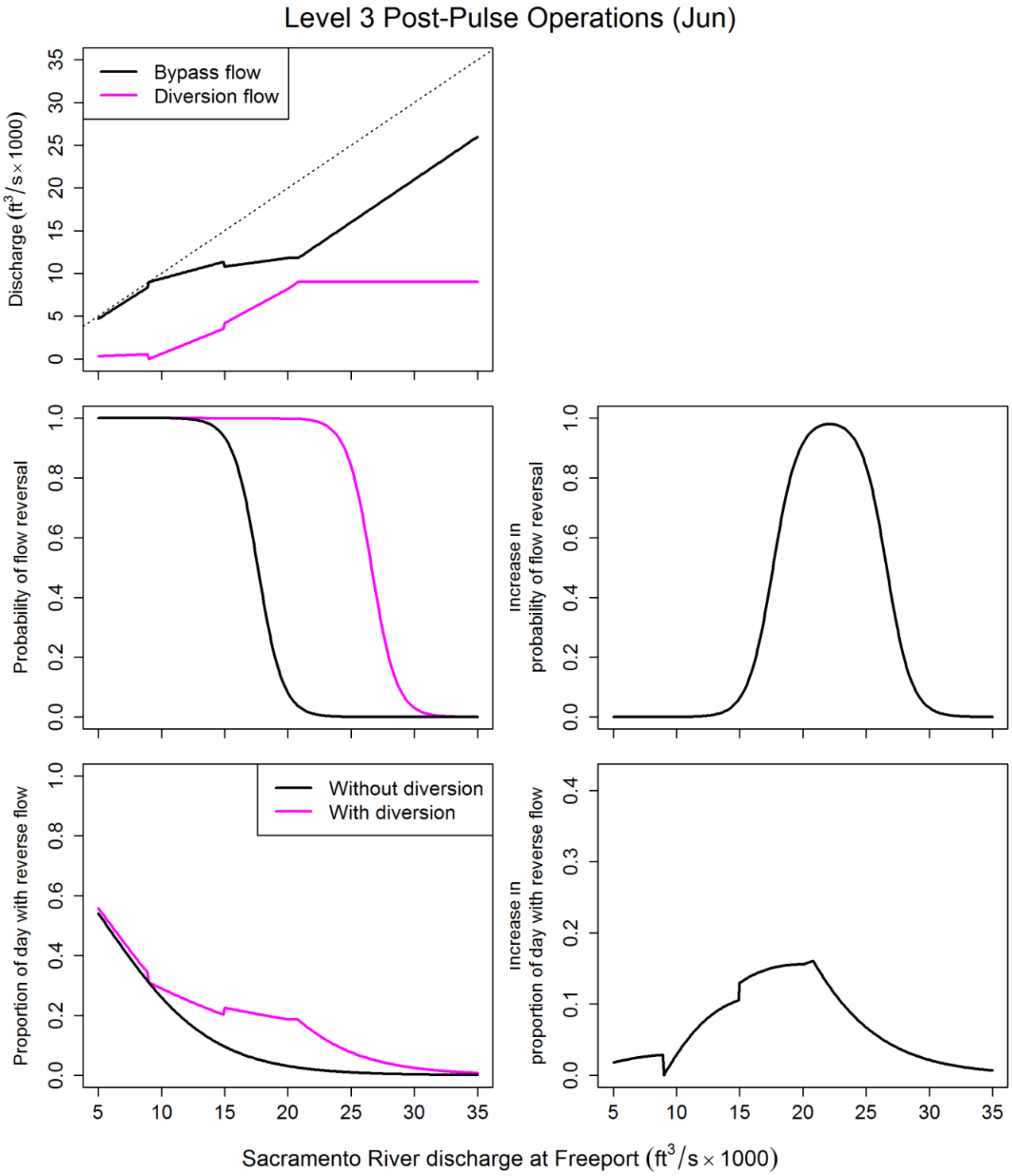

Figure 12. Effect of North Delta Diversion (NDD) on bypass discharge, probability of flow reversal, and proportion of the day with reverse flow for Level 3 post-pulse operations in June as defined in the NDD bypass rules. In the top panel, the dotted line shows bypass discharge when diversion discharge is zero.

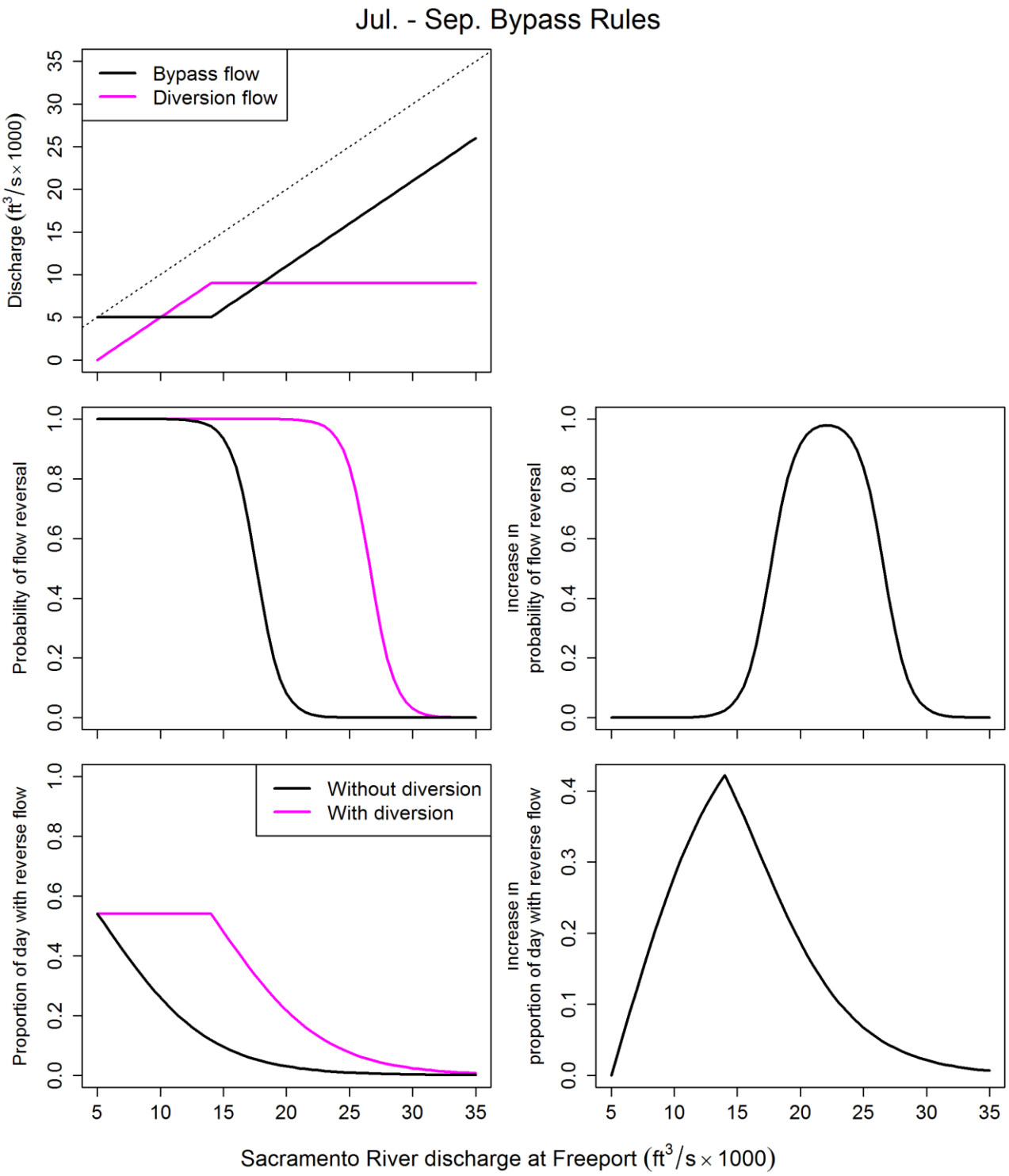

Figure 13. Effect of North Delta Diversion (NDD) on bypass discharge, probability of flow reversal, and proportion of the day with reverse flow for July–December as defined in the NDD bypass rules. In the top panel, the dotted line shows bypass discharge when diversion discharge is zero.

Discussion

The NDD bypass rules are designed to allow for diversion of water from the Sacramento River while providing fish protection during peak migration periods into the Delta. Low level pumping, which is initiated following flow pulses that have been shown to initiate migration of juvenile winter-run Chinook salmon (del Rosario and others, 2013), limits diversion to 10% of the maximum diversion capacity (9,000 ft^3/s). Under this criterion, we found little increase in the proportion of day with reverse flow (fig. 2), and therefore we expect little increase in entrainment of juvenile salmon into Georgiana Slough. In contrast, we found that the duration of flow reversal could be increased considerably during periods when juvenile salmon are likely to be migrating past Georgiana Slough. The conditions under which the P_{day}(reverse) can increase by ≥10 percentage points between October and June include October–November bypass rules and level 3 post-pulse operations from December through June (see lower right panels of fig. 3, 6, 9, and 12).

We performed our analysis under the assumption that the North Delta Diversion was operated at a constant rate for an entire day and followed the NDD bypass rules based on daily mean flows of the Sacramento River at Freeport. It is generally understood that the diversion would be operated "in real time" to prevent reverse flows at Georgiana Slough. However, to evaluate the effect of "real time" operations on flow reversal requires clear definition of control rules governing how the diversion would be operated to control flow reversals. To our knowledge, such control rules have yet to be developed and evaluated using tools such as DSM2. Consequently, our analysis evaluates the effect of the NDD bypass rules on flow reversals based on the how the rules were explicitly written according to readily available information on a daily basis (i.e., Sacramento River flows at Freeport).

Although it is unclear how real-time operations would be implemented, it is conceivable that the diversion could be operated on an hourly basis, in concert with the tides, to increase diversion during ebb tides but restrict diversion during flood tides. Such operations would likely require detailed real-time predictions of tides and tidally varying river flow in order to account for variation in tidal cycles that affect the frequency, magnitude, and duration of reverse flows at a given Freeport discharge. The relationship between Sacramento River inflows with the probability of flow reversal and proportion of the day with reverse flow is driven by tidal cycles that vary on hourly and biweekly time scales. Spring and neap cycles cause variation in the strength of the tides, which drives variation in the mean river flows at which the Sacramento River reverses downstream of Georgiana Slough. For example, at a Freeport discharge of 7,500 ft^3/s the proportion of the day with reverse flow ranges from about 0.12 to 0.35. This variation is driven by spring and neap tides that vary on biweekly scales, with strong spring tides corresponding with longer duration of reverse flows and weak neap tides corresponding with shorter duration of reverse flow. Based on these considerations, if real-time operations are to be used to control flow reversals, we strongly encourage development of explicit control rules for real-time management and testing of these controls through simulation models such as DSM2.

Bias Correction of DSM2 Discharge Predictions at the Junction of Sacramento River with the Delta Cross Channel and Georgiana Slough

Introduction

We used the fish entrainment model described in Perry and others (2015) to simulate the probability of fish entering Georgiana Slough and the Delta Cross Channel under the California Water Fix scenarios simulated by DSM2 (Delta Simulation Model 2), a one dimensional hydrodynamic

simulation model of the Delta (http://baydeltaoffice.water.ca.gov/modeling/deltamodeling/models/dsm2/dsm2.cfm). Because the model of Perry and others (2015) used USGS gage flows in the Sacramento River and Georgiana slough to predict routing of juvenile salmon, we evaluated how well DSM2 predicted USGS gage flows. The concern was that bias in DSM2 flow predictions would induce bias in the predicted routing probabilities.

We found evidence of bias when DSM2 flow predictions at USGS gages at Georgiana Slough (GEO; USGS Gage 11447903) and Sacramento River below Georgiana Slough (WGB; USGS Gage 11447905) was compared to the observed flows data. Therefore, we used observed discharge data collected at these sites from November 2006 to December 2011 to correct discharge values predicted by DSM2. Discharge over this time period ranged from -8,440 to 21,000 ft^3/s at WGB and -534 to 8,300 ft^3/s at GEO. It is important to note that although DSM2 version 8.1.2 is the current release version, DSM2 simulations for the California Water Fix used DSM2 version 8.0.6 to maintain consistency with the simulations conducted under the Bay Delta Conservation Plan. Although not presented here, we found DSM2 version 8.1.2 exhibited less bias when used to predict discharge at these gaging stations. By using observed flow data to correct DSM2 flow predictions, we eliminated any potential bias in routing probabilities that would result from using biased flow predictions to predict routing probabilities.

Methods

We developed two multiple linear regression models to predict observed flow at GEO and WGB as a function of DSM2 flows at WGA (Sacramento River Above the Delta Cross Channel), DCC (Delta Cross Channel), GEO, and WGB. Two indicator variables were evaluated; first, an indicator variable (I_{WGB}) was used to provide the direction of flow at WGB (upstream flow=1; downstream flow=0) and second, DCC_{gate} was used to indicate the status of the DCC gates (open=1, closed=0). Interactions between covariates were also included within the model. The model that resulted in the highest coefficient of determination (R^2) and met all assumptions of linear regression (i.e. homogeneity of residuals, low skew and kurtosis etc.) was selected as the best fit model. Lagged DSM2 flows were used to improve tidal phase shift. Alternative models were assessed to evaluate whether lagged flow variables improved model fit. Variables were lagged by 15 minute time steps from 15 minutes to 150 minutes.

Results

The best fit model for the GEO gaging station included flow at all four flow gages (WGA,WGB, GEO, and DCC) lagged by two time steps or 30 minutes (table 2). The indicator variable I_{WGB} and DCC gate position parameter (DCCgate) were included in the final model as main effects. The final model also included two- and three-way interactions. Two- and three-way interactions included the interactions between lagged flow at each flow station and DCC gate operation (DCCgate) and the interactions between lagged flow at each flow station and the flow indicator parameter I_{WGB}. The interaction between the indicator variable I_{WGB} and DCC gate position was also retained in the final model. Three-way interactions consisted of the interactions between lagged flow at each flow station, DCC gate position, and the flow indicator variable I_{WGB}. The model fit the observed data reasonably well (fig. 14). Residuals between predicted and observed discharge at GEO were normally distributed and centered near zero. Coefficient of determination (R^2) was 0.949.

The model for the WGB gaging station was similar to the model used to correct flows at GEO, however flows were lagged by three time steps or 0.75 hour (i.e., $Q_{GEO,3}$; table 3). All flow stations, the flow indicator parameter, and the DCC_{gate} indicator were included as main effects in the model (table 2).

Two- and three-way interactions were also included in the final model. Two-way interactions retained in the final model consisted of the interactions between flow at each flow station and DCC gate position. The interaction between flow at WGA, WGB, and GEO and the flow indicator variable I_{WGB} was also retained. The flow indicator variable interacted with gate operations was also retained in the final model. Three-way interactions consisted of flow at WGA, WGB, and GEO interacted with the DCC gate operations and the flow indicator parameter. The model provided a good fit to the data (R^2=0.962) and residuals between corrected flow and observed flow were normally distributed and had a mean of approximately zero for all model fits (fig. 15).

Table 2. Parameter estimates for correction of flow at GEO. Parameters were lagged by 2 time steps or 30 minutes. The second subscript in each parameter indicates the number of lag steps.

[Q, discharge; GEO, Georgiana Slough; WGB, Sacramento River below Walnut Grove; WGA, Sacramento River above Walnut Grove; DCCgate, indicator variable for position of the Delta Cross Channel gate position (1 = open, 0 = closed); I, indicator variable for flow direction at WGB (1 = upstream, 0 = downstream)]

	Parameter	Estimate	Std. Error
Main Effects	(Intercept)	-81.800	4.616
	$Q_{GEO,2}$	0.568	0.009
	$Q_{WGB,2}$	-0.099	0.007
	$Q_{WGA,2}$	0.238	0.007
	$Q_{DCC,2}$	-0.152	0.010
	I_{WGB}	894.100	21.910
	DCCgate	219.600	8.072
Two-way interactions	$Q_{GEO,2}$*DCCgate	-0.731	0.016
	$Q_{WGB,2}$*DCCgate	-0.296	0.011
	$Q_{WGA,2}$*DCCgate	0.330	0.012
	$Q_{DCC,2}$ *DCCgate	-0.195	0.014
	I_{WGB} *DCCgate	-483.200	24.150
	$Q_{GEO,2}$ * I_{WGB}	-0.148	0.026
	$Q_{WGB,2}$ * I_{WGB}	-0.050	0.020
	$Q_{WGA,2}$ * I_{WGB}	-0.015	0.022
	$Q_{DCC,2}$ * I_{WGB}	-0.111	0.024
Three-way interactions	$Q_{GEO,2}$ * I_{WGB} * DCCgate	0.220	0.032
	$Q_{WGB,2}$ * I_{WGB} * DCCgate	0.203	0.023
	$Q_{WGA,2}$ * I_{WGB} * DCCgate	-0.209	0.025
	$Q_{DCC,2}$ * I_{WGB} * DCCgate	0.333	0.027

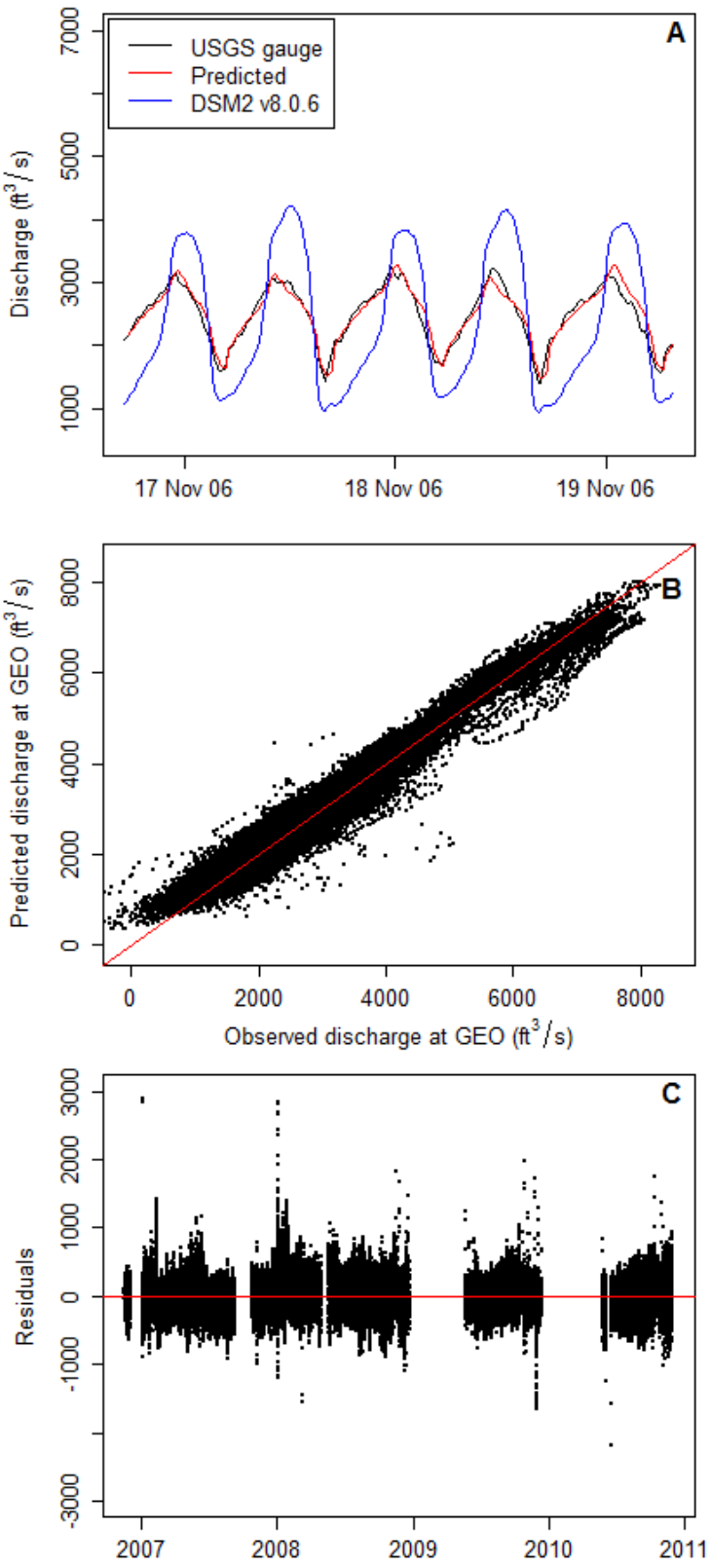

Figure 14. Comparison of observed, DSM2v8.0.6, and regression-corrected (predicted) discharge at the Georgiana Slough (GEO) USGS flow gage (*A*). Panel B compares observed and predicted discharge. The

diagonal line has slope of 1 and an intercept of zero. Residuals of the predicted and observed discharge for GEO (*C*).

Table 3. Parameter estimates for correcting DSM2v8.0.6 predicted flow at WGB. Parameters were lagged by 3 times steps or 0.75 hour. The second subscript in each parameter indicates the number of lag steps.
[Q, discharge; GEO, Georgiana Slough; WGB, Sacramento River below Walnut Grove; WGA, Sacramento River above Walnut Grove; DCCgate, indicator variable for position of the Delta Cross Channel gate position (1 = open, 0 = closed); I, indicator variable for flow direction at WGB (1 = upstream, 0 = downstream)]

	Parameter	Estimate	Std. Error
Main Effects	(Intercept)	-2317	22
	$Q_{GEO,3}$	2.326	0.039
	$Q_{WGB,3}$	2.173	0.030
	$Q_{WGA,3}$	-1.283	0.033
	$I_{WGB,3}$	1392	87
	DCCgate,3	722	38
	$Q_{DCC,3}$	1.447	0.042
Two-way interactions	$Q_{GEO,3}$ * DCCgate,3	0.678	0.065
	$Q_{WGB,3}$ * DCCgate,3	1.002	0.042
	$Q_{WGA,3}$ * DCCgate,3	-1.055	0.045
	I_{WGB} * DCCgate,3	-394	99
	$Q_{GEO,3}$ * $I_{WGB,3}$	-0.314	0.052
	$Q_{WGB,3}$ * $I_{WGB,3}$	0.017	0.038
	$Q_{WGA,3}$ * $I_{WGB,3}$	-0.349	0.041
	$Q_{DCC,3}$ * DCCgate,3	1.219	0.051
Three-way interactions	$Q_{GEO,3}$ * I_{WGB}*DCCgate,3	-0.491	0.082
	$Q_{WGB,3}$ * I_{WGB}*DCCgate,3	-0.263	0.042
	$Q_{WGA,3}$ * I_{WGB}*DCCgate,3	0.256	0.045

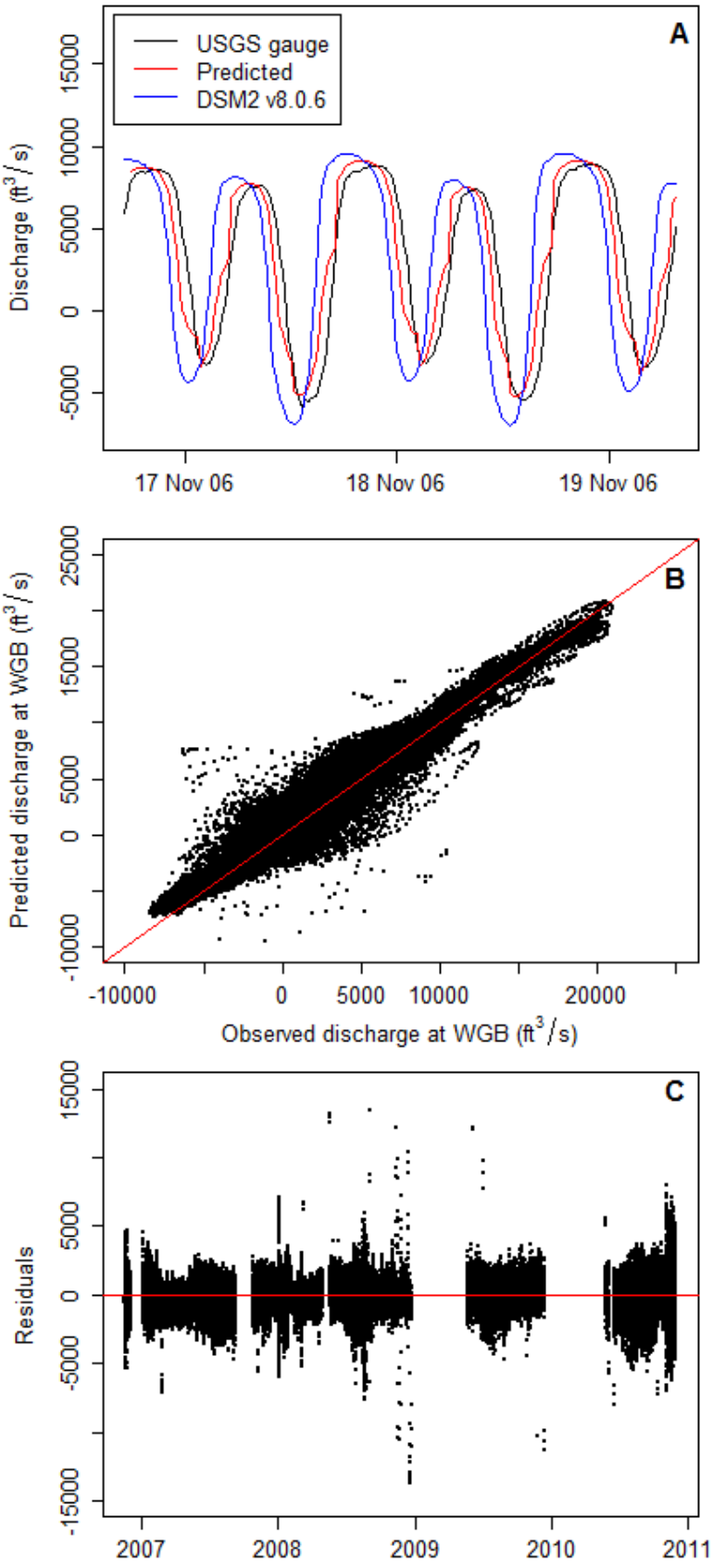

Figure 15. Comparison of observed, DSM2v8.0.6, and regression-corrected (predicted) discharge at the

Sacramento River below Walnut Grove (WGB) USGS flow gage (A). Panel B compares observed and predicted discharge. The diagonal line has slope of 1 and an intercept of zero. Panel (C) illustrates the residuals of the predicted and observed discharge for WGB.

Discussion

We used lagged flow variables in conjunction with indicator variables to create models to adjust DSM2 predicted flows at both GEO and WGB. Our models provide a good adjustment for correcting the DSM2 output; however the predictive power of our model is limited to the range of flows used for the correction. Empirical data were only available for the 2006–2011 time period. Therefore, one should use caution in applying the model to predict flows outside of the range of flows used in the model development.

Interestingly, lags in the model covariates improved model fits, suggesting that DSM2 8.0.6 does not adequately predicting tidal phasing at this location. Given the time lags it appears that DSM2 is predicting water pulses to arrive later than observed at WGB and earlier than observed at GEO. In addition DSM2 routinely overestimated the magnitude of flow at WGB. In contrast, DSM2 did accurately estimate the magnitude of flow at GEO. This suggests the complex hydrodynamics at this junction are not fully captured by DSM2.

Simulating the Effect of the North Delta Diversion on Daily Entrainment Probability of Juvenile Chinook Salmon into Georgiana Slough and the Delta Cross Channel

Introduction

This analysis investigates the effect of the proposed North Delta Diversion on entrainment of juvenile Chinook salmon into Georgiana Slough and the Delta Cross Channel. Specifically, we used the entrainment probability model of Perry and others (2015) to predict entrainment probabilities from flows simulated by DSM2 under the California Water Fix No Action Alternative (NAA) and Proposed Action (PA) from October to June for each water year in the 82-year simulation period (ICF International 2016). The entrainment model is based on a multinomial regression analysis that estimated the probability (π) of individual fish entering the Delta Cross Channel (π_{DCC}), Georgiana Slough (π_{GEO}), and the Sacramento River (π_{SAC}) from three variables: 1) instantaneous river discharge (i.e., measured every 15 minutes) entering Georgiana Slough (GEO), 2) instantaneous discharge of the Sacramento River below Georgiana Slough (WGB), and 3) Delta Cross Channel gate position (1 = open, 0 = closed). The entrainment model was based on acoustic telemetry data collected between 2006 and 2009 from 919 juvenile late-fall Chinook salmon that passed the river junction over rivers flows of the Sacramento River at Freeport ranging from 6,802 ft^3/s to 40,700 ft^3/s. A complete description of the model, including model equations, estimated parameters, and goodness-of-fit, can be found in Perry and others (2015) and Perry (2010).

Methods

To apply the entrainment model of Perry and others (2015) to DSM2 output, we 1) corrected DSM2 discharge simulations at WGB and GEO using the regression correction described in the

previous section, 2) formed covariates required for the entrainment model from the corrected DSM2 discharge simulations, and 3) simulated route entrainment probabilities for the entire 82-year time series of 15-minute flows simulated under the NAA and PA scenarios. We then tabulated daily entrainment probabilities as the mean of 15-minute entrainment probabilities for each day. Daily entrainment probabilities represent the expected fraction of fish entering each channel on a particular date under the assumption that fish migrate past this river junction uniformly over the diel period.

The entrainment model was based on data collected at a maximum Freeport discharge of 40,700 ft^3/s, whereas the DSM2 simulations include Freeport flows up to about 80,000 ft^3/s. Therefore, we evaluated the model's behavior at flows >40,000 ft^3/s because we were concerned about using the entrainment model outside the range of data used to inform the model. Simulated daily entrainment probabilities based on DSM2 output increased from about 0.35 to 0.50 as Freeport discharge increased from about 40,000 ft^3/s to 80,000 ft^3/s (fig. 16). We compared these predictions to estimates from Perry and others (2014), who quantified the effect of a non-physical barrier on entrainment into Georgiana Slough when Freeport flows were approximately 80,000 ft^3/s. At this flow level, Perry and others (2014) estimated a mean entrainment probability into Georgiana Slough of about 0.30 with the non-physical barrier off, as opposed to 0.50 simulated using the Perry and others (2015) model. This finding suggests that entrainment probabilities remain relatively constant at flows between 40,000 ft^3/s and 80,000 ft^3/s rather than increasing as the model of Perry and others (2015) would predict. Because the Perry and others (2015) model appears to over-estimate entrainment at high flows, we restricted our analysis of simulated daily entrainment probabilities to flows at Freeport ≤ 41,000 ft^3/s.

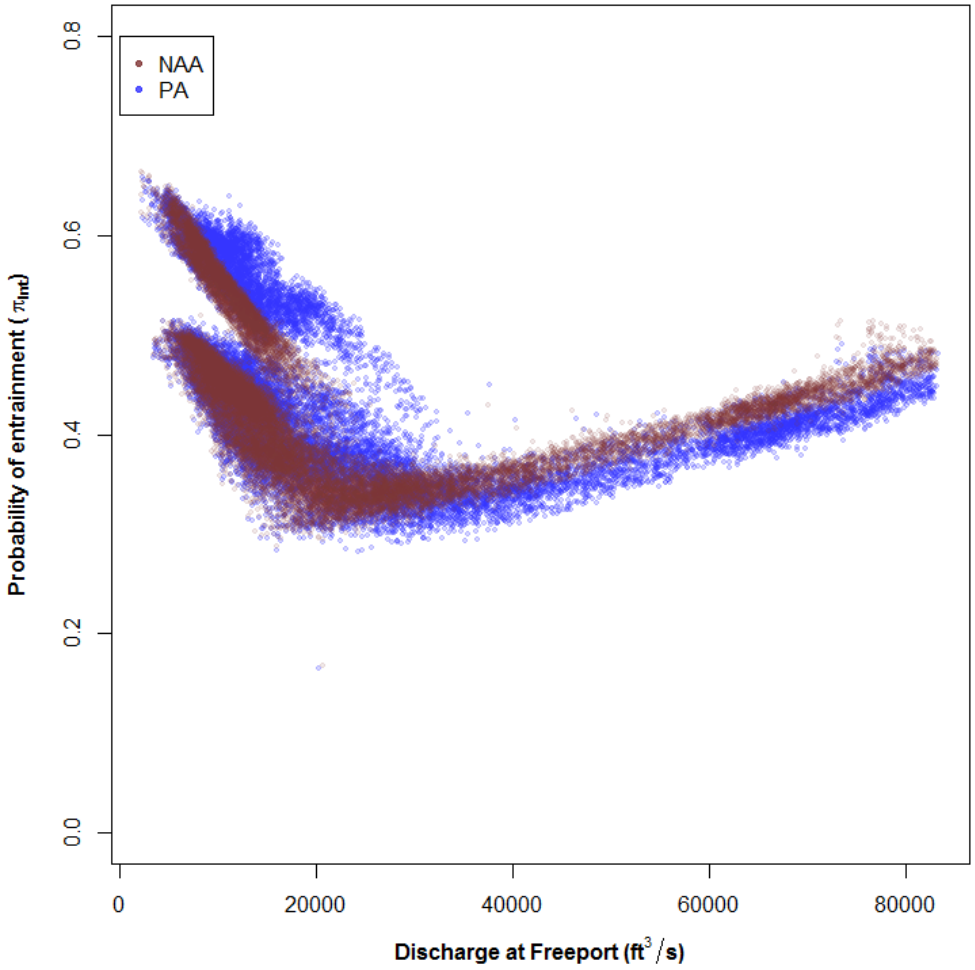

Figure 16. Daily probability of entering the interior Delta ($\pi_{Int} = \pi_{GEO} + \pi_{DCC}$) as a function of Sacramento River discharge at Freeport for the No Action Alternative (NAA) and Proposed Action (PA) simulations conducted with DSM2 (Delta Simulation Model 2).

Ideally, if daily inflows to the Delta were the same between NAA and PA scenarios, then daily entrainment probabilities could be compared directly among common dates that employ different management alternatives between scenarios. However, daily inflows to the Delta vary between scenarios owing to upstream flow management that differs between scenarios, making direct comparison of daily entrainment probabilities problematic. Therefore, we compared scenarios by summarizing daily entrainment probabilities within each year by averaging daily entrainment probabilities over 1) each year, 2) each month within years, and 3) over three alternative run-timing distributions. Summary statistics included days when Freeport flows were ≤41,000 ft^3/s and excluded days when flows were >41,000 ft^3/s. The three run-timings were: 1) a uniform distribution, where an equal proportion of fish out-migrated each month; 2) an early run timing representing winter-run Chinook in years when flow conditions trigger an early migration into the Delta and 3) a late run timing representing winter-run Chinook in years when the migration begins in December (fig. 17). Estimates of annual entrainment probability for the different run timings were calculated as a weighted average of the daily entrainment probability weighted by the proportion of the run migrating on a given day. Run

timing distributions were based on juvenile trapping data from Knight's landing (Yvette Redler, written commun. January 7, 2016). We then categorize these annual statistics according to California Department of Water Resources water-year classification and compare box plots of annual entrainment probabilities for different water year types. CDWR uses five classifications for water year type in the Sacramento Valley that are based on water year index value (WYI): W=Wet, WYI ≥ 9.2; AN=above normal, 7.8 ≤ WYI ≤ 9.2; BN=Below Normal, 6.5≤ WYI ≤7.8; D=Dry, 5.4≤ WYI ≤6.5; C=Critical, WYI ≤ 5.4.

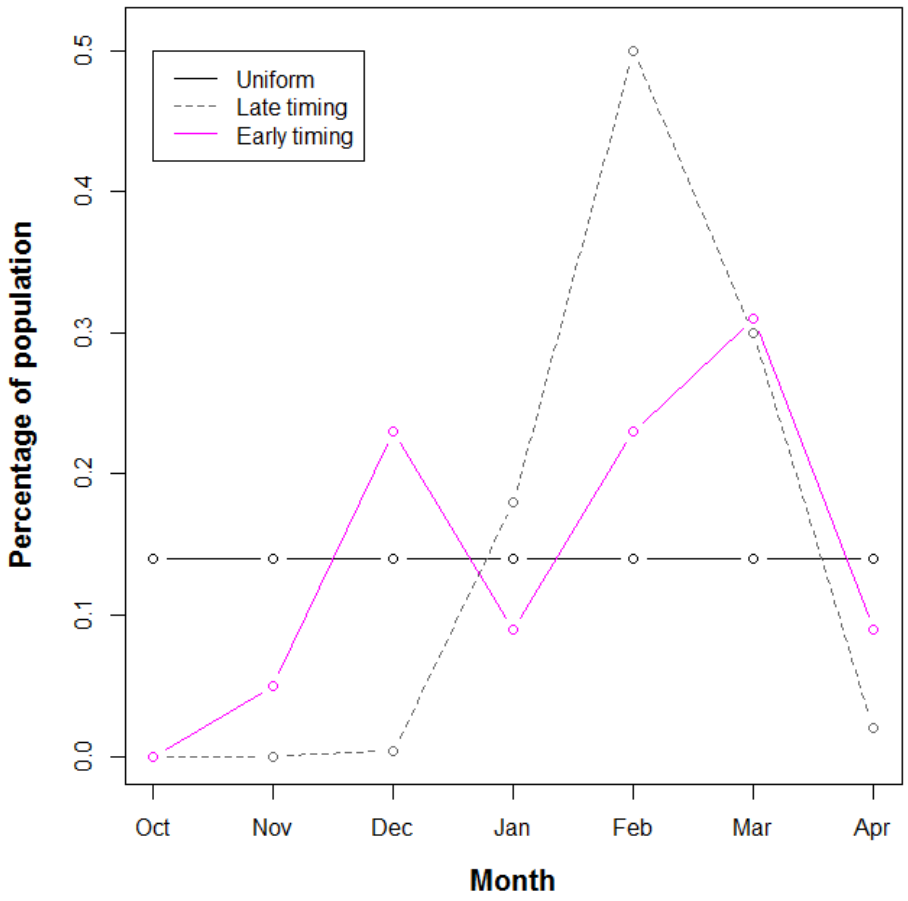

Figure 17. Migration timing scenarios used to estimate mean annual entrainment probabilities, with the early and late timings representing two scenarios for winter-run Chinook salmon in the Sacramento River.

Results

We estimated entrainment probabilities for NAA and PA under three run timing distributions over an 82-year period. In general, the mean annual entrainment probabilities differed little between PAA and NA (table 4); however, we found small but consistent differences in entrainment between scenarios that varied across years (figs. 18 and 19). For example, under uniform run timing, the annual probability of fish remaining in the Sacramento River for the PA scenario was 0 to 4 percentage points lower than under the NAA scenario, indicating higher entrainment into the interior Delta (fig. 18). Mean annual entrainment into the Delta Cross Channel was consistently higher under the PA scenario,

but differences in mean annual entrainment into Georgiana Slough exhibited both positive and negative deviations (fig. 18). These findings indicate that the increased entrainment into the Delta Cross Channel was responsible for the lower probability of fish remaining in the Sacramento River.

Table 4. Mean (SD) predicted annual entrainment probabilities under different run-timing scenarios for No Action Alternative (NAA) and Proposed Action (PA) simulations conducted with DSM2.

	Sacramento River		Georgiana Slough		Delta Cross Channel	
Run-timing	NAA	PA	NAA	PA	NAA	PA
Uniform	0.571 (0.031)	0.556 (0.028)	0.349 (0.017)	0.346 (0.017)	0.072 (0.03)	0.089 (0.024)
Late	0.555 (0.132)	0.547 (0.129)	0.344 (0.09)	0.352 (0.094)	0 (0)	0 (0)
Early	0.558 (0.085)	0.549 (0.082)	0.346 (0.061)	0.352 (0.063)	0.018 (0.018)	0.021 (0.018)

The differences in entrainment under the early run timing revealed a slightly higher (by about 1 percentage point) mean annual probability of entering the Delta Cross Channel (fig. 19). However, for the late run timing, we found little difference in entrainment between the NA and PAA scenarios (fig. 19). The differences in annual entrainment among the run timing scenarios suggested that daily entrainment probabilities varied seasonally, thereby affecting annual entrainment differentially for the alternative run timings.

Examination of the distribution of mean monthly entrainment probabilities revealed seasonal patterns that varied among water year types (fig. 20). In all but critically dry years, median π_{SAC} (the probability of fish remaining in the Sacramento River) under the PA scenario was up to 5 percentage points lower than under the NAA scenario for October and November (fig. 20). This difference was also apparent for June in wet years. Because the early and late run timings had zero probability of migrating in October and low (early) or zero (late) probability of migrating in November, these run timing distributions had little exposure to the differences in operation between PA and NAA during these months, leading to little difference in mean annual entrainment probabilities (figs. 18 and 19).

For the months of October, November, and June, fish had a lower probability of remaining in the Sacramento owing primarily to a higher probability of entering the Delta Cross Channel. We also found that the Delta Cross Channel gates were open more frequently in October and November (fig. 21), which likely contributed to the higher mean monthly probability of entering the Delta Cross Channel. For example, we identified days when the Delta Cross Channel was open under PA but closed under NAA (fig. 22). Under NAA the DCC remained closed owing to NDD Bypass flows > 25,000 ft^3/s, a trigger that causes closure of the DCC (fig. 22). However, under PA, water diversion reduced bypass flows below 25,000 ft^3/s, which allowed the DCC gates to remain open (fig. 22). In turn, opening the Delta Cross Channel gates substantially reduced the instantaneous probability of fish remaining in the Sacramento River by increasing the probability of fish entering the Delta Cross Channel (fig. 22).

We found that much of the interannual variation in mean annual entrainment probabilities could be attributed to water year classification. For example, mean annual π_{SAC} for the uniform run timing decreased from a median of about 0.60 to 0.52 as water year type transitioned from wet to critically dry years (fig. 23). In contrast, both mean annual π_{GEO} and π_{DCC} increased as water years transitioned from wet to critically dry (fig. 23). Between scenarios, π_{SAC} under PA was less than under the NAA scenario for all water year types for a uniform run timing (fig. 24). For the early and late run timings, we observed little difference between PA and NAA for π_{SAC} for wet and above normal water years, but π_{SAC} was consistently lower for PA relative NAA (fig. 24). Although we found some consistent differences between PA and NAA among water year types, the median difference between scenarios was <2 percentage points for all mean annual entrainment probabilities.

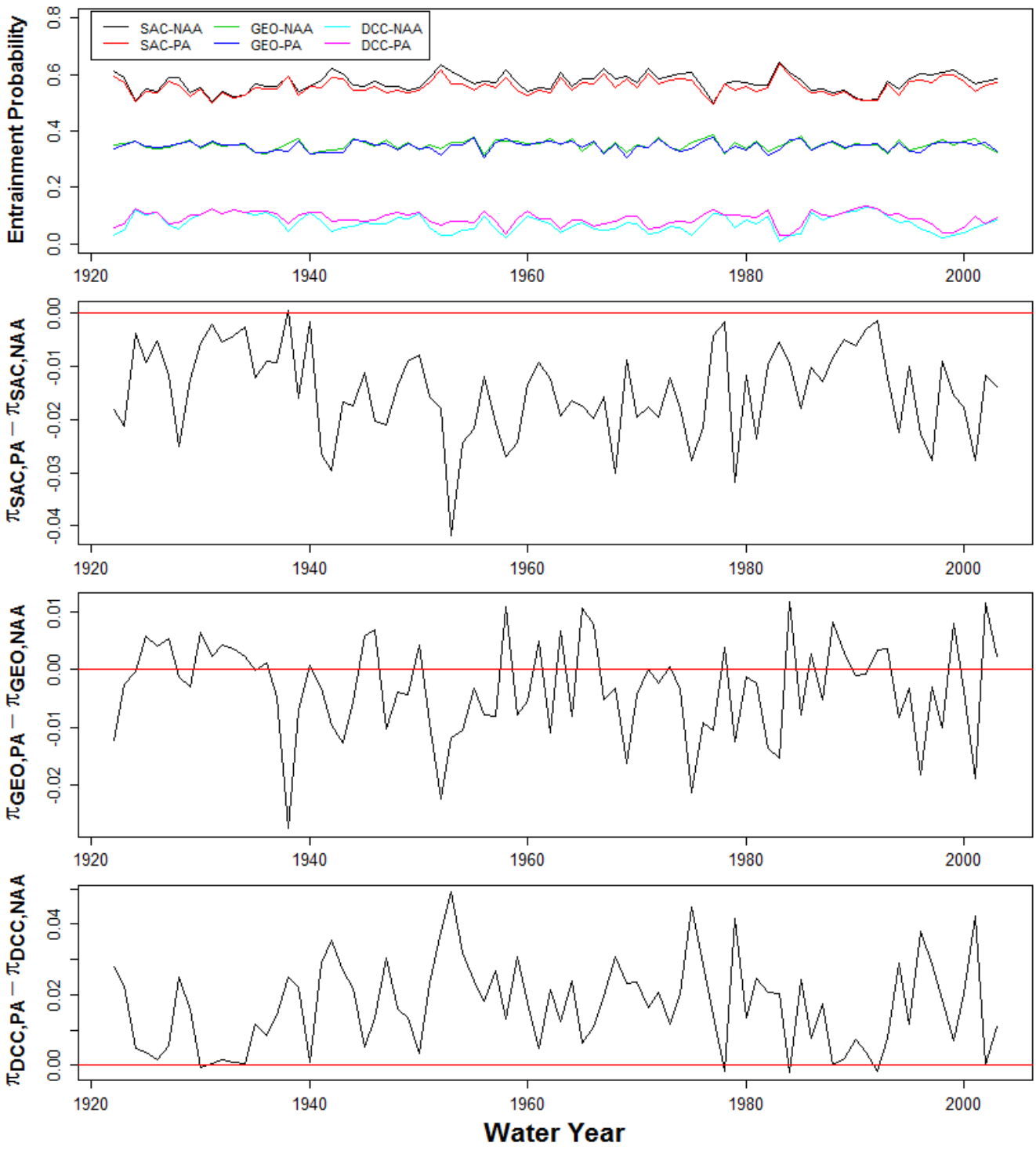

Figure 18. Comparison of predicted mean annual entrainment probability assuming uniform run timing for the Sacramento River (SAC), Georgiana Slough (GEO), and Delta Cross Channel (DCC) between the Proposed Action (PA) and No Action Alternative (NAA). Shown are the mean annual entrainment probabilities (top panel) and the difference in entrainment between scenarios for SAC, GEO, and DCC (lower panels). Values above the horizontal red line indicate greater entrainment under the PA scenario.

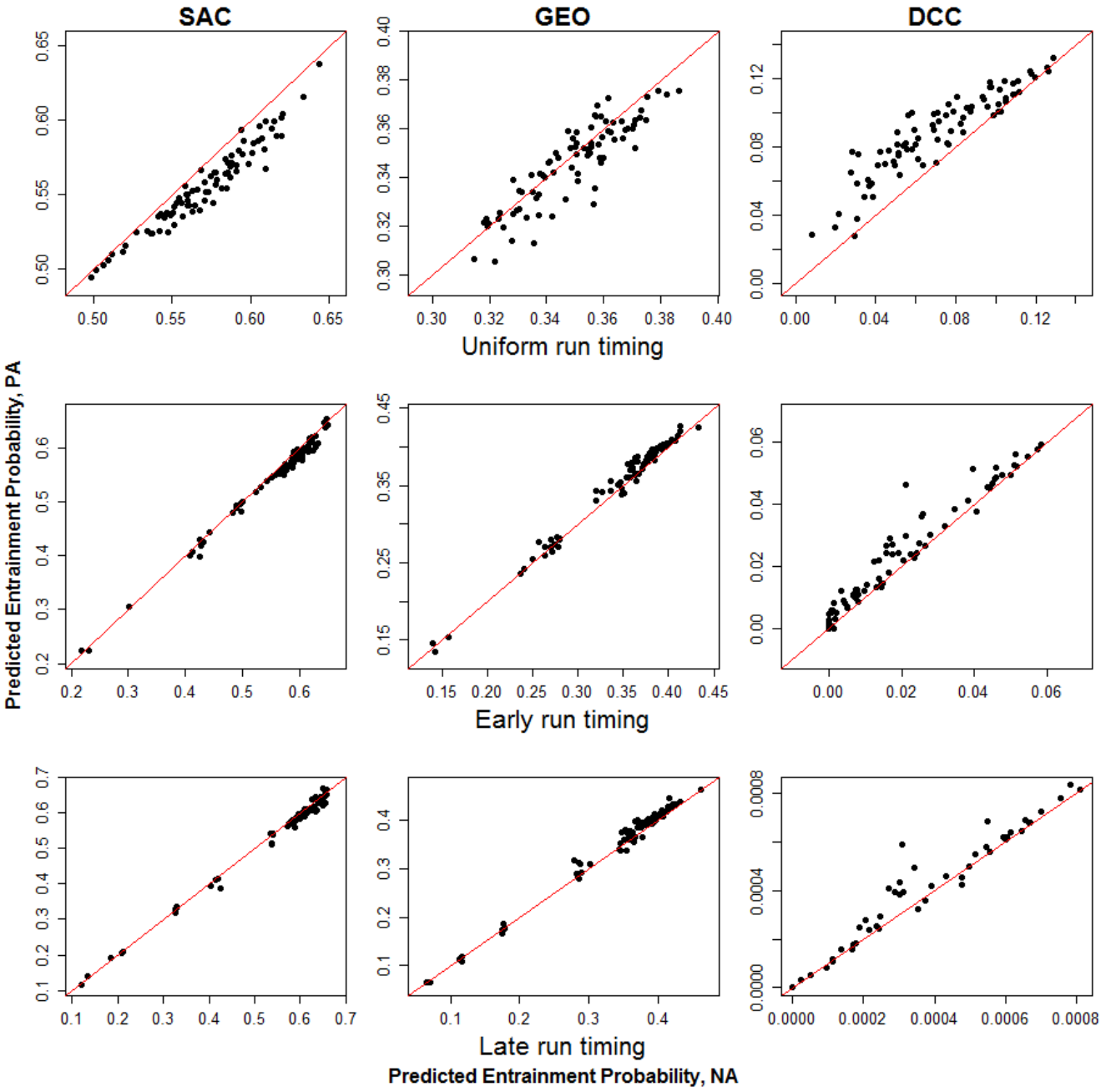

Figure 19. Comparison of predicted mean entrainment probability for the Sacramento River (SAC), Georgiana Slough (GEO), and Delta Cross Channel (DCC) between the Proposed Action (PA) and No Action Alternative (NAA) for uniform arrival and two different run timings for winter run Chinook salmon. The data points are paired by year, and the diagonal line has slope of one and an intercept of zero.

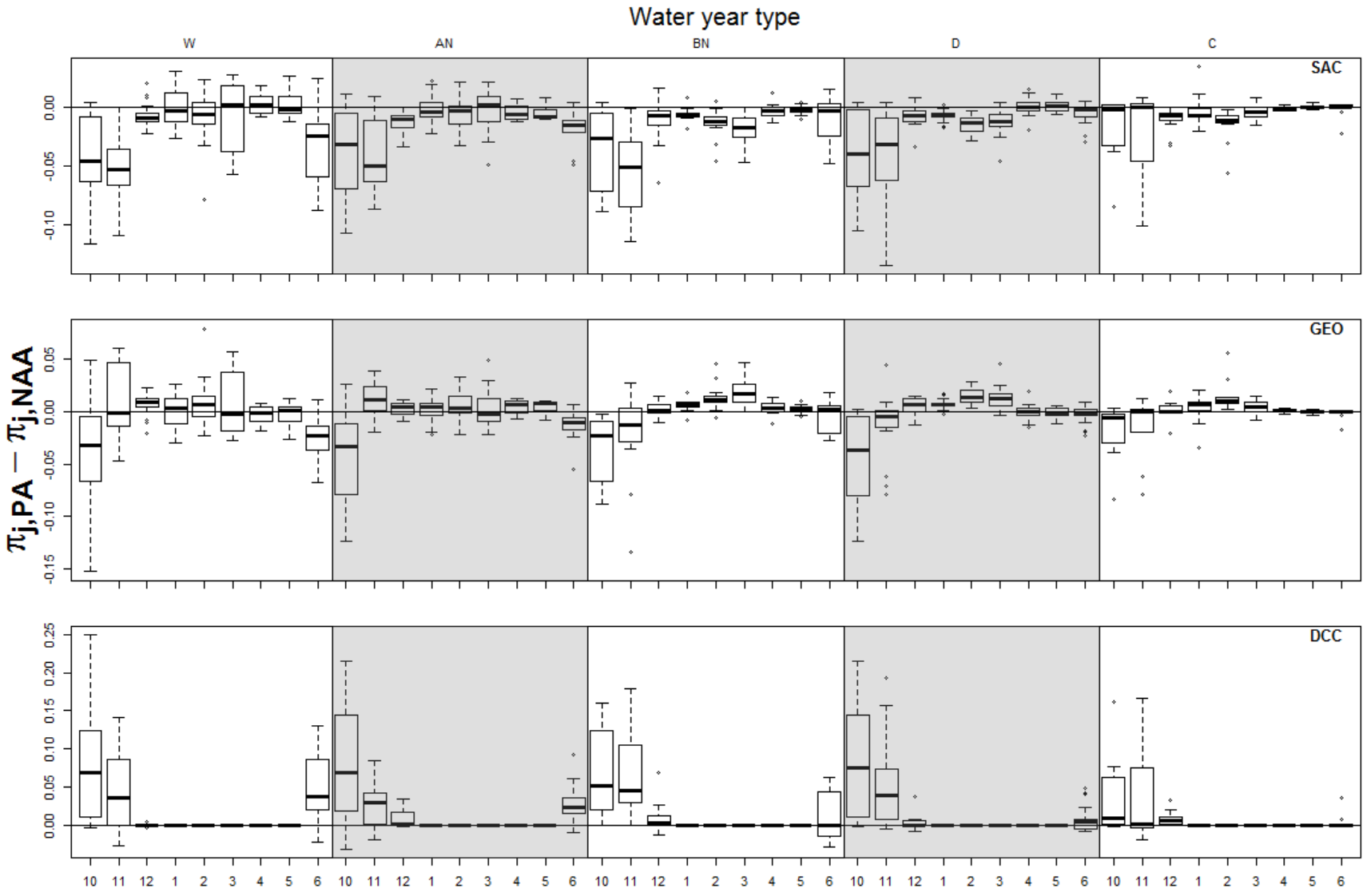

Figure 20. Boxplot of the difference predicted entrainment probability between the Proposed Action (PA) and No Action Alternative (NAA) by water year type and month assuming a uniform run timing (W=Wet, AN=Above Normal, BN=Below Normal, D=Dry, C=Critical). Boxes range from the 25th to the 75th percentiles with a line indicating the median, whiskers extend 1.5 times past the length of the box, and dots represent data points that fall beyond the whiskers.

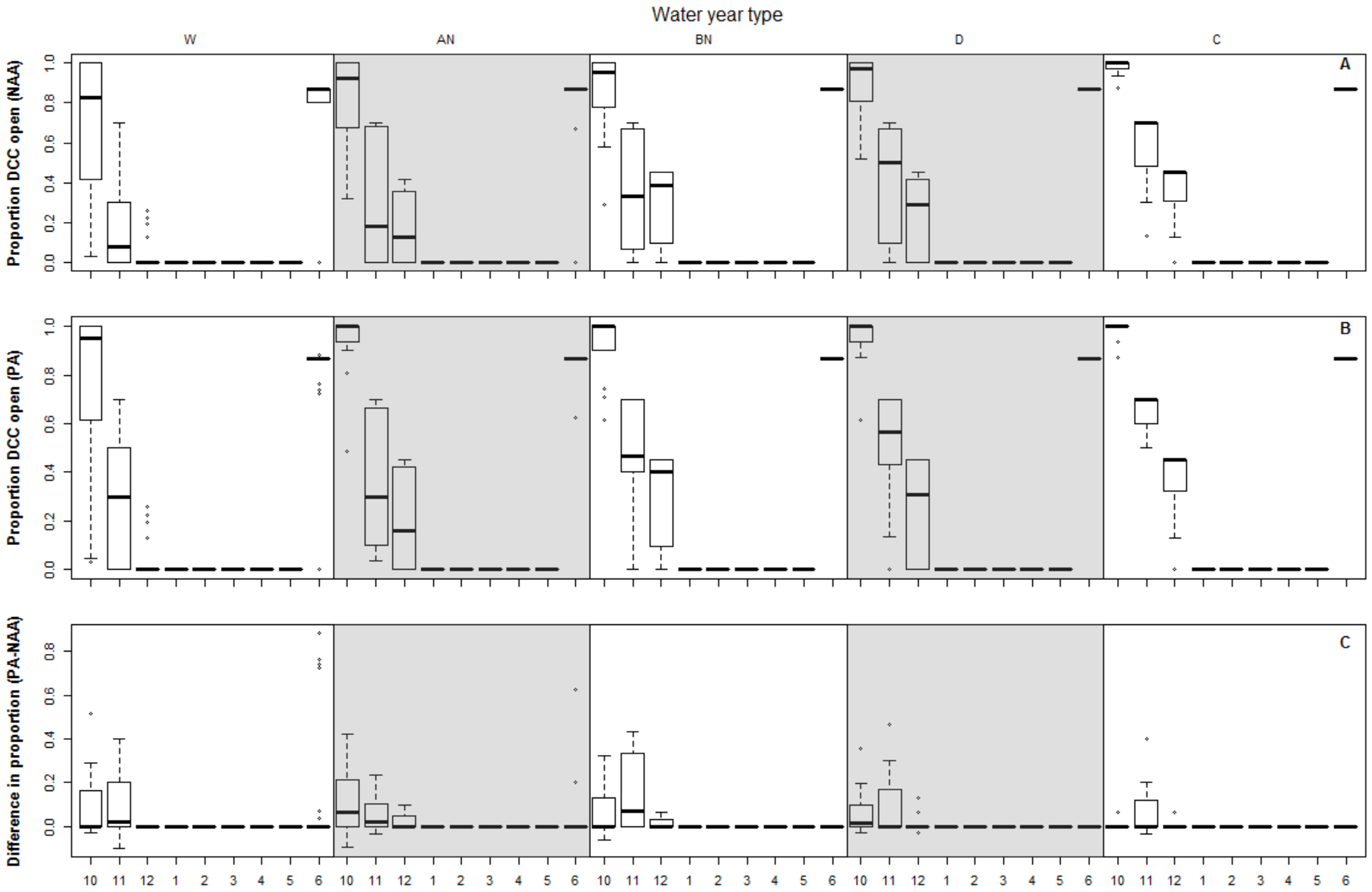

Figure 21. Boxplot of the proportion of each month that the DCC was open for the No Action Alternative (NAA, panel A), Proposed Action (PA, panel B), and the difference between PA and NAA (panel C) by water year type (W=Wet, AN=Above Normal, BN=Below Normal, D=Dry, C=Critical). Boxes range from the 25th to the 75th percentiles with a line indicating the median, whiskers extend 1.5 times past the length of the box, and dots represent data points that fall beyond the whiskers.

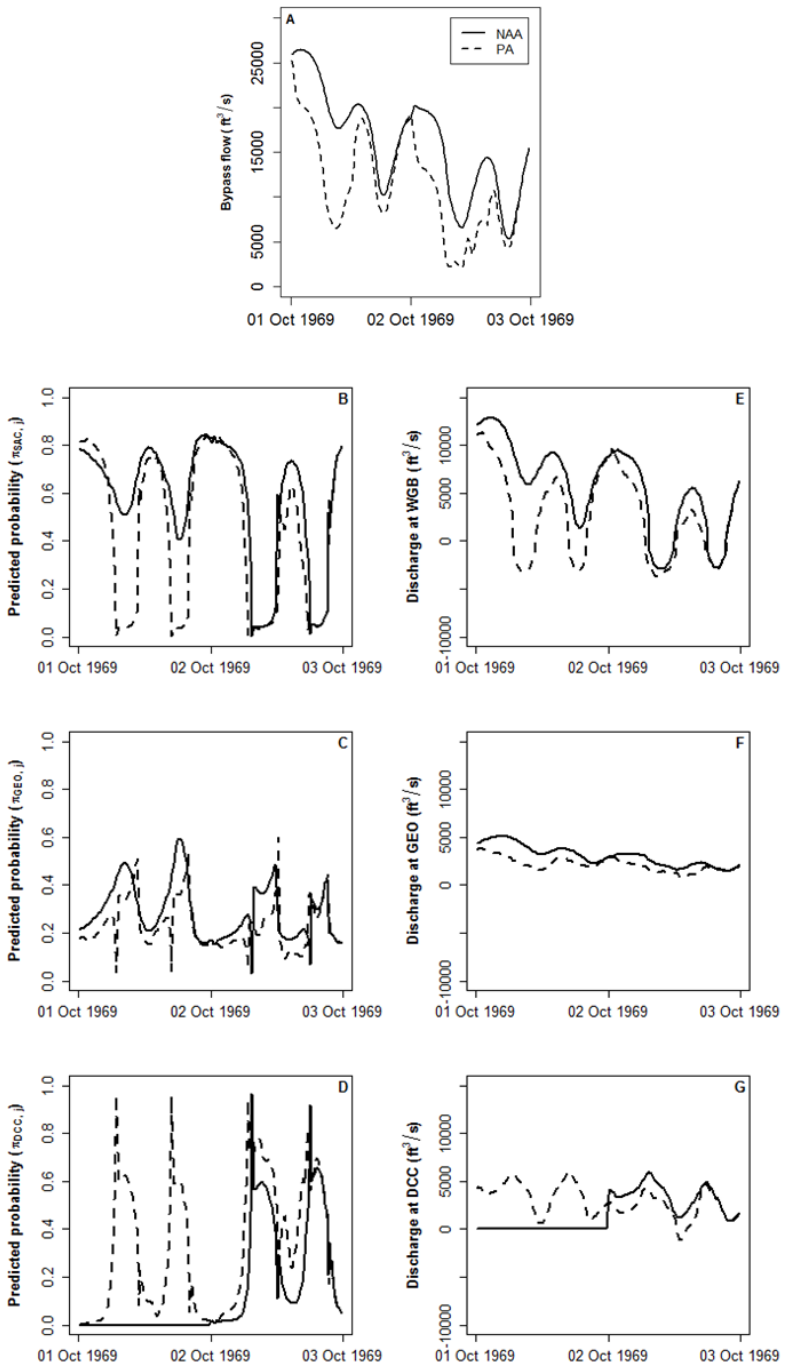

Figure 22. Comparison of bypass flows (A), predicted probability of entrainment into Sacramento River (B), Georgiana Slough (C), and the Delta Cross Channel (D) for the Proposed Action (PA) and No Action Alternative (NAA) during dates when the DCC was open under PA but closed under NAA. Discharge entering each route for NAA and PA are also shown (E, F, G).

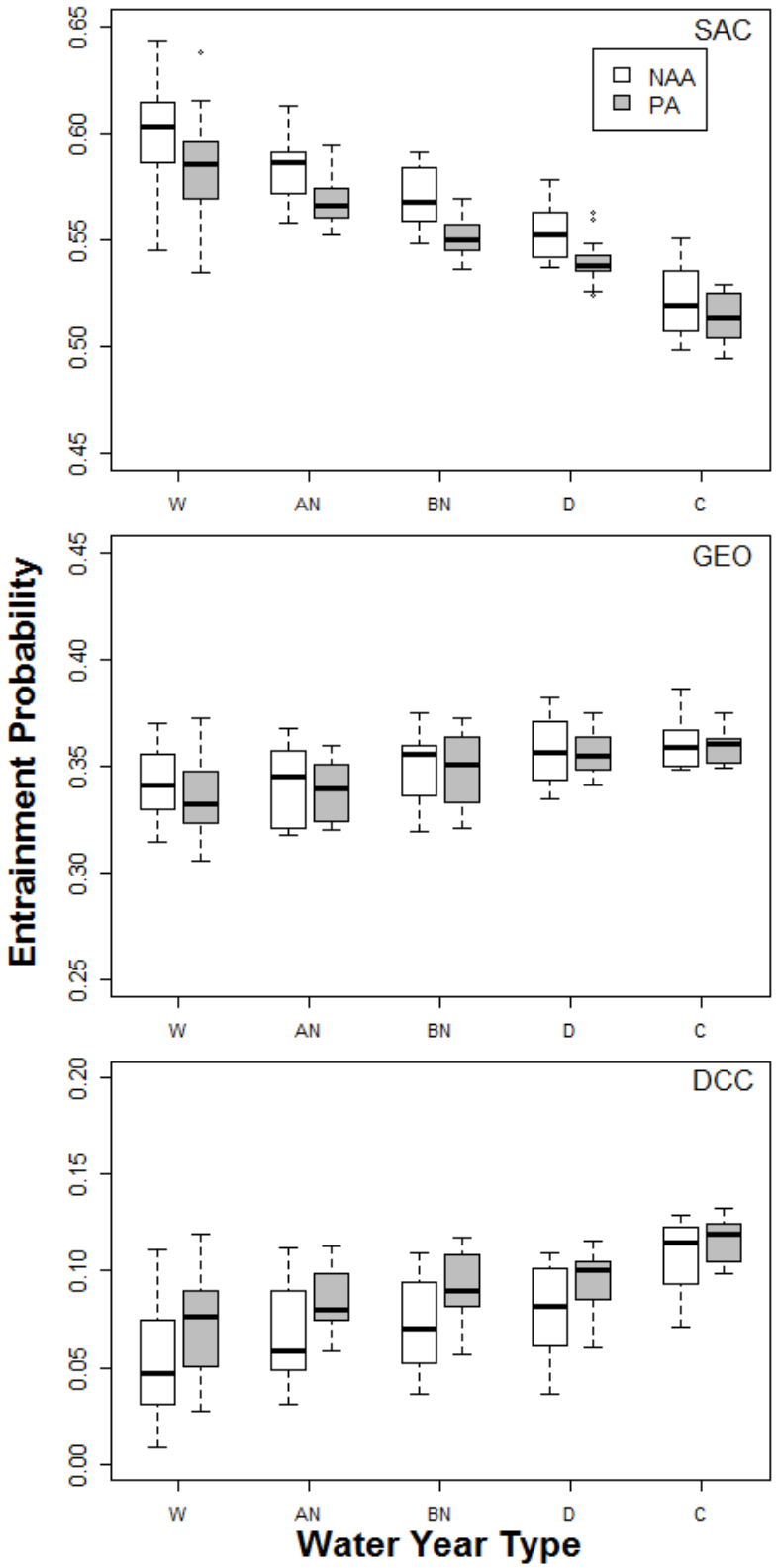

Figure 23. Boxplot of predicted mean annual entrainment probability for the Sacramento River (SAC), Georgiana Slough (GEO), and Delta Cross Channel (DCC) between the No Action Alternative (NAA) and Proposed Action (PA) by water year type based on a uniform run timing distribution (W=Wet, AN=Above Normal, BN=Below Normal,

D=Dry, C=Critical). Boxes range from the 25th to the 75th percentiles with a line indicating the median, whiskers extend 1.5 times past the length of the box, and dots represent data points that fall beyond the whiskers.

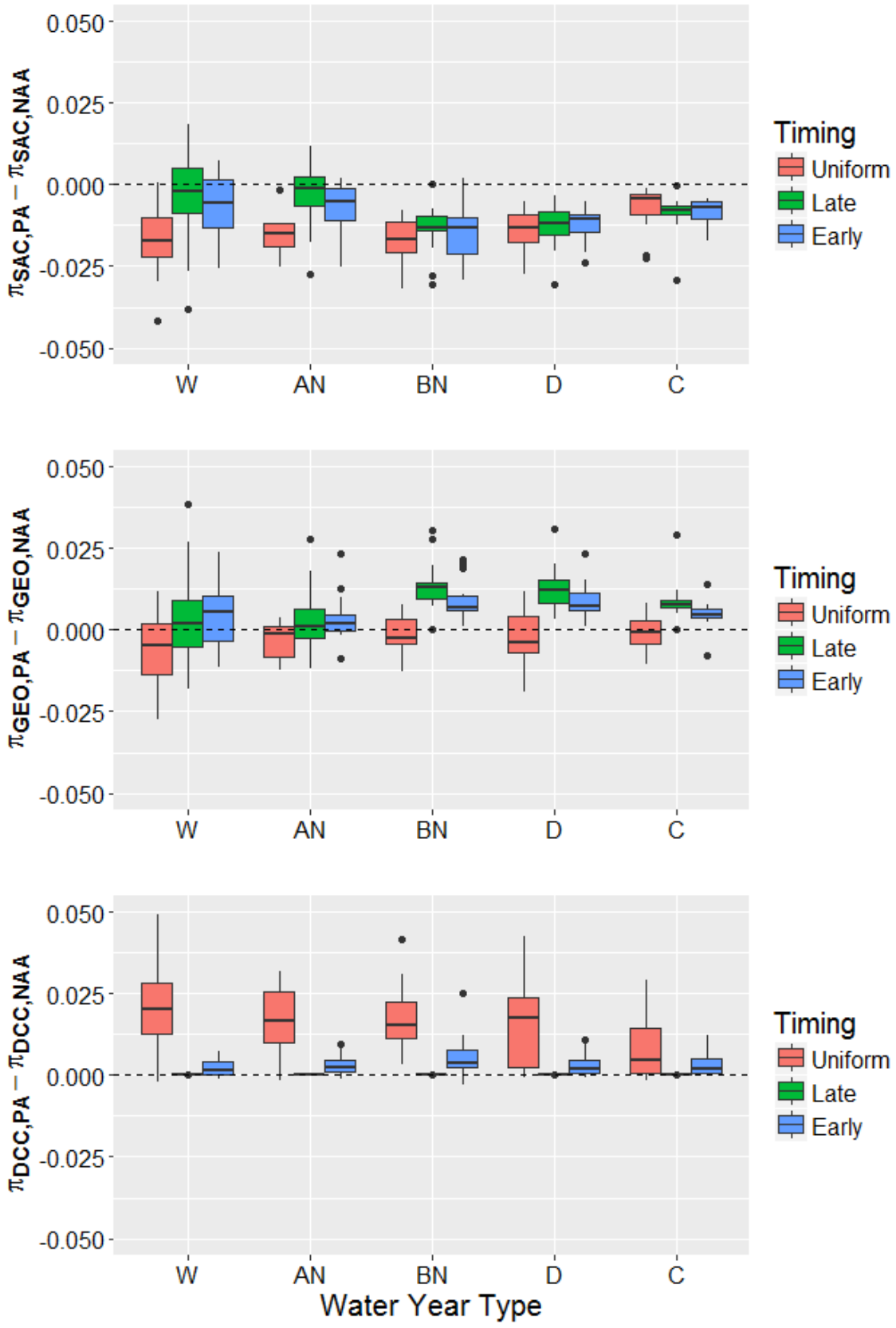

Figure 24. Boxplots of the difference between No Action Alternative (NAA) and Proposed Action (PA) for each

route (SAC = Sacramento River, GEO = Georgiana Slough, DCC = Delta Cross Channel) by water year type (W=Wet, AN=Above Normal, BN=Below Normal, D=Dry, C=Critical) and run timing scenario. Boxes range from the 25th to the 75th percentiles with a line indicating the median, whiskers extend 1.5 times past the length of the box, and dots represent data points that fall beyond the whiskers.

Discussion

We used previously developed entrainment models to predict the probability of fish entrainment into the interior Delta via Georgiana Slough and the Delta Cross Channel under the PA and NAA scenarios for different run timings and water year types. Overall the probability of remaining in the Sacramento River was lower under the PA scenario, but the magnitude of the difference was small. However, when run timing was assumed to occur between December and April, this difference was even less because fish were less exposed to periods when we observed the largest difference in entrainment between scenarios (October and November).

Although we observed relatively small differences in entrainment, we restricted our analysis to flows <41,000 ft^3/s to avoid potential bias in predicted entrainment probabilities at higher flows. When the entrainment model of Perry and others (2015) was used to predict entrainment at higher flows, the model predicted that entrainment increased with increasing river flow up to about 50% entrainment at flows of 80,000 ft^3/s at Freeport (fig. 16). However, comparison to estimates of entrainment from Perry and others (2014) at similar flows indicated entrainment into Georgiana Slough of only about 30%. The entrainment model was fit to data that encompassed the range of flows where the Sacramento River transitions from strongly reversing to non-reversing flows. Thus, the model's parameterization captures changes in entrainment owing to the strength of reversing flows, and revealed that highest entrainment occurred at the lowest flows where tidal forcing increases the magnitude and duration of reverse flows. The available empirical evidence suggests that entrainment stabilizes as inflows increase above the level at which reverse flows cease, but more data is needed to substantiate this observation. Assuming this pattern holds true, excluding the high-flow observations from our analysis would tend to weight the mean annual entrainment probabilities more towards the higher daily entrainment probabilities that occur at lower discharges. Therefore, we may have observed even less difference in mean annual entrainment probabilities between PA and NAA had we used a model that predicted daily entrainment probabilities are relatively constant at flows >41,000 ft^3/s.

The difference in entrainment between scenarios was primarily driven by the difference in operation of the DCC between PA and NAA. Under the PA scenario, the DCC was open more frequently, thus exposing more fish to being entrained into the interior Delta via the DCC. Two triggers require the DCC to close: 1) Flow below the NDD exceeding 25,000 ft^3/s and 2) flow at Wilkins Slough on the Sacramento River exceeding 7,500 ft^3/s. Water diversions have no effect on flow at Wilkins Slough, which leaves the flow below the diversion as the primary driver of the differences between entrainment under the PA and NAA scenarios. Diversions under the PA reduced the flow to below 25,000 ft^3/s, thus increasing the number of days the DCC could remain open. This was particularly evident in October and November during wet and above normal water year types when discharge above the diversion was greater than 25,000 ft^3/s. For example, under PA in October during wet years the DCC was open for about three more days than under the NAA scenario. During drier water year types, the DCC was operated similarly between PA and NAA since flows in those years rarely exceeded 25,000 ft^3/s. When the DCC was operated in a similar manner between scenarios (drier years), entrainment to the interior was higher due to the general relationship between flow and entrainment to the interior delta. Under lower flows entrainment to the interior delta is higher due to tidal forcing at the Georgiana Slough divergence.

Perry and others (2013) explored the sensitivity of overall survival of emigrating juvenile Chinook salmon to changes in entrainment into the interior Delta. This analysis found that completely eliminating entrainment to the interior Delta resulted in a 2–7 percentage point increase in overall survival through Delta, under the assumption of no change in route-specific survival. Thus, we expect that a 3-5 percentage point difference in the probability of being entrained to the interior Delta between PA and NAA would contribute relatively little to the change in overall survival. However, it is important to recognize that reduced inflows to the Delta owing to the NDD may simultaneously influence both route-specific survival and migration routing. Such simultaneous changes may result in larger expected changes in survival than the effect of routing alone on overall survival.

References Cited

DWR, 2013, Bay Delta Conservation Plan, Public Draft. Prepared by ICF International for California Department of Water Resources, Sacramento, CA.

ICF International. 2016. Biological Assessment for the California WaterFix. January. (ICF 00237.15.) Sacramento, CA. Prepared for United States Department of the Interior, Bureau of Reclamation, Sacramento, CA.

Perry, R.W., Skalski, J.R., Brandes, P.L., Sandstrom, P.T., Klimley, A.P., Ammann, A., and MacFarlane, B., 2010, Estimating survival and migration route probabilities of juvenile Chinook salmon in the Sacramento-San Joaquin River Delta: North American Journal of Fisheries Management, v. 30, p. 142–156.

Perry, R.W., Brandes, P.L., Burau, J.R., Klimley, A.P., MacFarlane, B., Michel, C., and Skalski, J.R., 2013, Sensitivity of survival to migration routes used by juvenile Chinook salmon to negotiate the Sacramento-San Joaquin River Delta: Environmental Biology of Fishes, v. 96, p. 381–392.

Perry, R.W., Romine, J.G., Adams, N.S., Blake, A.R., Burau, J.R., Johnston, S.V., and Liedtke, T.L. 2014. Using a non-physical behavioral barrier to alter migration routing of juvenile Chinook salmon in the Sacramento-San Joaquin River Delta. River Research and Applications. v. 30, p, 192–203.

Perry, R.W., Brandes, P.L., Burau, J.R., Sandstrom, P.T., and Skalski, J.R., 2015, Effect of tides, river flow, and gate operations on entrainment of juvenile salmon into the interior Sacramento-San Joaquin River Delta: Transactions of the American Fisheries Society, v. 144, p. 445–455.

del Rosario, R.B., Redler, Y.J., Newman, K., Brandes, P.L., Sommer, T., Reece, K., and Vincik, R., 2013, Migration patterns of juvenile winter-run-sized Chinook salmon (*Oncorhynchus tshawytscha*) through the Sacramento–San Joaquin Delta: San Francisco Estuary and Watershed Science v. 11, p. 1–22.

Appendix

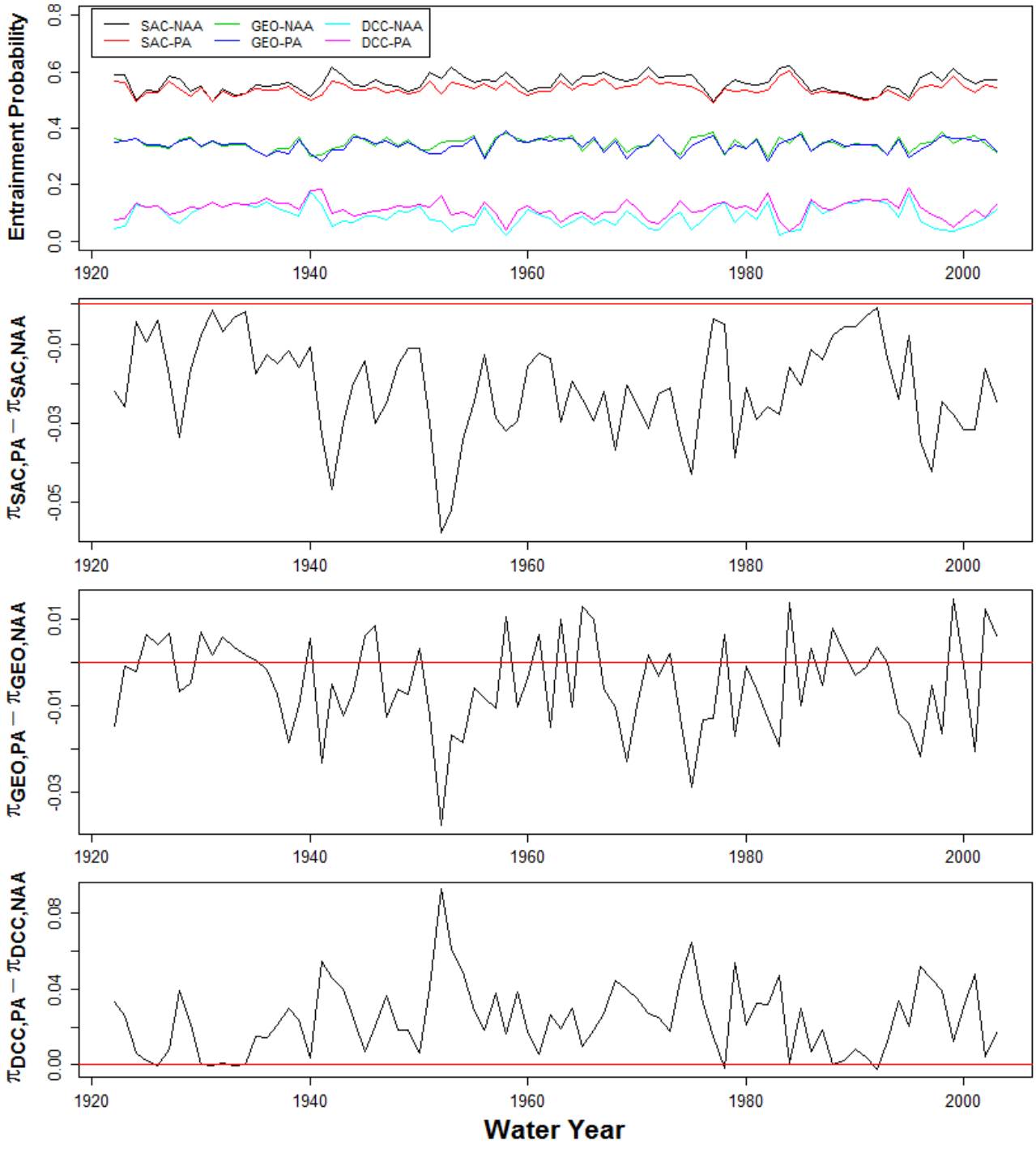

Figure 25. Comparison of predicted mean annual entrainment probability during daytime hours assuming uniform run timing for the Sacramento River (SAC), Georgiana Slough (GEO), and Delta Cross Channel (DCC) between the Proposed Action (PA) and No Action Alternative (NAA). Shown are the mean annual entrainment probabilities (top panel) and the difference in entrainment between scenarios for SAC, GEO, and DCC (lower panels). Values above the horizontal red line indicate greater entrainment under the PA scenario.

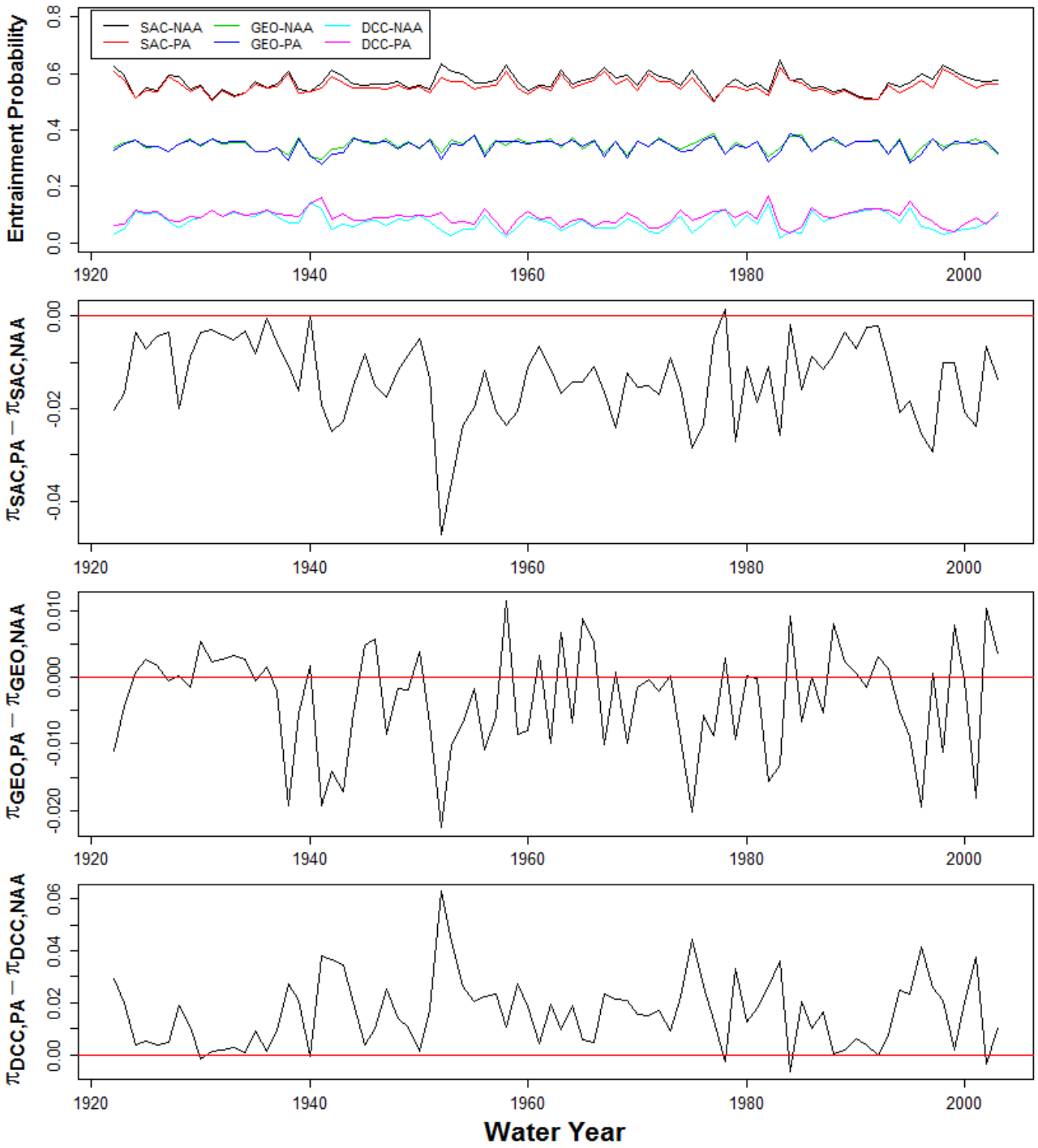

Figure 26. Comparison of predicted mean annual entrainment probability during nighttime hours assuming uniform run timing for the Sacramento River (SAC), Georgiana Slough (GEO), and Delta Cross Channel (DCC) between the Proposed Action (PA) and No Action Alternative (NAA). Shown are the mean annual entrainment probabilities (top panel) and the difference in entrainment between scenarios for SAC, GEO, and DCC (lower panels). Values above the horizontal red line indicate greater entrainment under the PA scenario.